NATIONAL TECHNICAL UNIVERSITY OF ATHENS-

SCHOOL OF NAVAL ARCHITECTURE AND MECHANICAL ENGINEERING

Diploma Thesis

“Thermo-economic assessment of a gas turbine combined system with alternative fuels for cruise vessel”

Athanasios G. Vallis

A.M.:21612

Research Advisor: Dr. Georgios Dimopoulos, Associate Professor

Athens

November, 2024

DECLARATION OF AUTHENTICITY / ZHTHMATA COPYRIGHT

The person who prepares the Diploma Thesis bears the entire responsibility for determining the fair use of the material, which is defined on the basis of the following factors: the purpose and nature of the use (commercial, non-profit or educational), the nature of the material used (part of the text, tables, figures, images or maps), the percentage and significance of its possible consequences on the market or the general value of the copyrighted text.

THREE-MEMBER COMMITTEE OF INQUIRY:

MEMBER A: Georgios Dimopoulos, Associate Professor

MEMBER B: Ioannis M. Prousalidis, Professor

MEMBER C: Dimitrios B. Liridis, Professor

Thanks

This diploma thesis was carried out at the Department of Marine Engineering of the School of Naval Architecture of NTUA during the academic year 2023 – 2024. First of all, I would like to thank my parents and my family in general for their valuable help and support. I would also like to thank Professor Dr. George Dimopoulos for his valuable guidance and assistance.

Contents

Table of Figures

Tables

Abstract

The need to reduce greenhouse gas emissions in the shipping industry has stimulated the exploration of technological alternatives to align with increasingly stringent regulations, primarily through the adoption of low or zero-carbon fuels. Although gas turbines have demonstrated their ability to be a proven solution in marine applications, they are presently confined to specialized in ship segments like naval vessels and fast ferries. The use of gas turbines for oceangoing merchant and passenger ships has been limited, mainly due to their lower efficiency when compared to traditional marine diesel engines. The landscape, however, is evolving with the push for decarbonization, as gas turbines can efficiently utilize alternative fuels like bio or synthetic natural gas, methanol, and hydrogen. The successful introduction of gas turbines into future commercial vessels will rely on two key factors: a) a substantial increase of the overall efficiency achieved through the utilization of combined cycle steam turbine power generation (COGES), and b) the ability to competitively use alternative fuels. This work investigates a marine gas turbine combined cycle concept aiming at efficiency levels that either match or surpass those of traditional marine diesel engines. Additionally, it is explored the integration of alternative fuels, such as natural gas, methanol, and hydrogen, with a focus on assessing the potential benefits in reducing CO_2 emissions. Employing a state-of-the-art process modeling tool and adopting a systems engineering approach, it is modeled and simulated the gas turbine combined cycle concept. The heat transfer in the heat recovery steam generation section is analyzed in detail and a new heat transfer model for the part-loads is proposed. Subsequently, the optimal operating parameters of the combined system are examined and a parametric analysis is performed on a wide load range for the studied alternative fuels. Then, a case study is carried out for the use of the examined system together with conventional diesel engines for the electrical demands of a modern cruise ship. Specifically, a plan for the simultaneous use of conventional diesel engines and COGES is created to maintain high levels of efficiency on a wide range of loads. Finally, the results of the case study are presented, which demonstrate that the proposed propulsion installation can combine the high efficiency levels of modern diesel engines with the use of alternative zero carbon fuels and can lead to significant levels of CO2 emission reduction.

Περίληψη

Η ανάγκη μείωσης των εκπομπών αερίων του θερμοκηπίου στη ναυτιλιακή βιομηχανία έχει τονώσει τη διερεύνηση τεχνολογικών εναλλακτικών λύσεων για την εναρμόνιση με όλο και πιο αυστηρούς κανονισμούς, κυρίως μέσω της υιοθέτησης καυσίμων χαμηλών ή μηδενικών εκπομπών άνθρακα. Παρόλο που οι αεριοστρόβιλοι έχουν αποδείξει την ικανότητά τους να αποτελούν αποδεδειγμένη λύση σε θαλάσσιες εφαρμογές, επί του παρόντος περιορίζονται σε εξειδικευμένα τμήματα πλοίων όπως πολεμικά πλοία και ταχύπλοα πλοία. Η χρήση αεριοστροβίλων για ποντοπόρα εμπορικά και επιβατηγά πλοία έχει περιοριστεί, κυρίως λόγω της χαμηλότερης απόδοσής τους σε σύγκριση με τους παραδοσιακούς ναυτικούς κινητήρες ντίζελ. Η ανάγκη όμως για απαλλαγή από τον άνθρακα τους καθιστά αναγκαίους, καθώς οι αεριοστρόβιλοι μπορούν να χρησιμοποιήσουν αποτελεσματικά εναλλακτικά καύσιμα όπως απλό ή συνθετικό φυσικό αέριο, μεθανόλη και υδρογόνο. Η επιτυχής εισαγωγή αεριοστροβίλων σε μελλοντικά εμπορικά πλοία θα βασιστεί σε δύο βασικούς παράγοντες: α) σημαντική αύξηση της συνολικής απόδοσης που επιτυγχάνεται μέσω της χρήσης της παραγωγής ηλεκτρικής ενέργειας με ατμοστρόβιλους συνδυασμένου κύκλου (COGES) και β) την ικανότητα ανταγωνιστικής χρήσης εναλλακτικών καυσίμων. Αυτή η εργασία διερευνά μια έννοια συνδυασμένου κύκλου ναυτικών αεριοστροβίλων με στόχο την επίτευξη επιπέδων απόδοσης που είτε ταιριάζουν είτε ξεπερνούν εκείνα των παραδοσιακών ναυτικών κινητήρων diesel. Επιπλέον, διερευνάται η ενσωμάτωση εναλλακτικών καυσίμων, όπως το φυσικό αέριο, η μεθανόλη και το υδρογόνο, με έμφαση στην αξιολόγηση των πιθανών οφελών από τη μείωση των εκπομπών CO_2. Χρησιμοποιώντας ένα σύγχρονο εργαλείο μοντελοποίησης διεργασιών και υιοθετώντας μια προσέγγιση μηχανικής συστημάτων, μοντελοποιείται και προσομοιώνεται η έννοια του συνδυασμένου κύκλου αεριοστροβίλου. Αναλύεται λεπτομερώς η μεταφορά θερμότητας στο τμήμα της παραγωγής ατμού μέσω ανάκτησης απορριπτόμενης θερμότητας και προτείνεται ένα νέο μοντέλο μειωμένης μεταφοράς θερμότητας για τα μερικά φορτία. Στη συνέχεια, διερευνώνται οι βέλτιστες παράμετροι λειτουργίας του συνδυασμένου συστήματος σε μερικά φορτία και πραγματοποιείται παραμετρική ανάλυση σε πλήρες εύρος φορτίου για 5 εναλλακτικά καύσιμα. Στη συνέχεια, πραγματοποιείται μελέτη περίπτωσης για τη χρήση του εξεταζόμενου συστήματος μαζί με συμβατικούς κινητήρες diesel για τις ηλεκτρικές απαιτήσεις ενός σύγχρονου κρουαζιερόπλοιου. Συγκεκριμένα, δημιουργείται ένα πλάνο χρήσης για τους συμβατικούς πετρελαιοκινητήρες και το COGES για τη διατήρηση υψηλών επιπέδων απόδοσης σε ένα πλήρες εύρος φορτίων. Τέλος, παρουσιάζονται τα αποτελέσματα της μελέτης περίπτωσης, τα οποία καταδεικνύουν ότι η προτεινόμενη εγκατάσταση πρόωσης μπορεί να συνδυάσει τα υψηλά επίπεδα απόδοσης των σύγχρονων πετρελαιοκινητήρων με τη χρήση εναλλακτικών καυσίμων μηδενικού άνθρακα και μπορεί να οδηγήσει σε σημαντικά επίπεδα μείωσης των εκπομπών CO2.

1. Introduction

In this work, the application of a heat recovery system to a marine gas turbine on a cruise ship was studied. The waste heat came from the gas turbine exhaust gas, which passed through an exchanger before being released to the environment. The combined system is called COGES and its individual parts will be analyzed in the next chapters, The aim of the work was initially the modeling of the COGES system and the optimization of its operating parameters in software. Then for the optimized COGES system, the aim was to study the achieved gas turbine fuel savings, carbon dioxide emissions reduction and thermal efficiency using various alternative fuels, which could not be used with a conventional marine diesel engine. Additionally, the objective was to compare the COGES system with conventional diesel engines in a full range of loads regarding the mentioned parameters.

Maritime transport dominates international trade, with approximately 80% of global trade by volume conducted via sea routes[1]. It is also responsible for around 796 million tons of CO2 emissions, accounting for 2.2% of total global greenhouse gas emissions, according to the 3rd IMO GHG Study[2]. It is predicted that growing global energy demands and economic development will cause CO2 emissions from shipping to increase by 50% to 250% by 2050, potentially reaching 12% to 18% of allowable CO2 emissions. In 2011, the IMO implemented mandatory measures to improve ship energy efficiency at the 62nd Marine Environment Protection Committee (MEPC) meeting. These included the Energy Efficiency Design Index (EEDI) for new ships and the Ship Energy Efficiency Management Plan (SEEMP) for operational ships, effective from January 1, 2013, for ships weighing 400GT and above[3]. At MEPC 72 in 2018, the IMO set a new strategy aiming to reduce greenhouse gas (GHG) emissions by 40% by 2040 and at least 50% by 2050, compared to 2008 levels. To achieve this, the IMO introduced new regulations, including the Attained Energy Efficiency Existing Ship Index (EEXI) and the annual Carbon Intensity Indicator (CII)[4]. The EEXI measures a ship's efficiency compared to a baseline, requiring vessels of 400GT and over to meet minimum standards. The CII sets an annual reduction factor to ensure continuous improvement in a ship's operational carbon intensity, based on a specific rating level. The need to improve the efficiency of the propulsion installation of ships and to reduce emissions with the aim of harmonizing with statutory rules leads shipping companies and the international research community to search for new technologies.

Mallouppas et al.[5] outlines several methods for improving fuel efficiency and reducing emissions in maritime vessels. It is mentioned that reducing vessel speed, especially through "slow steaming," lowers fuel consumption but increases transportation time. Hull resistance can be minimized by cleaning, using specialized coatings, and optimizing ship design. Another solution is the air lubrication systems, like bubble drag reduction, which reduce water resistance improving further efficiency. A fast-growing technology are the waste heat recovery (WHR) systems that exploit energy from exhaust gases and other heat sources to generate auxiliary power, offering fuel savings of 4–16.

Inal et al.[6] examines alternative zero-carbon fuels, particularly hydrogen and ammonia, for powering ships. It assesses these fuels against five key criteria: safety, cost, storage, sustainability, and environmental impact, using expert weightings determined through the Analytic Hierarchy Process. Safety and environmental impact emerge as the most significant factors. Ammonia shows a slight advantage over hydrogen, indicating its potential as a key fuel for achieving zero-carbon shipping. A sensitivity analysis was conducted to validate the reliability of the results.

Cullinane and Yang [7] examines the cost implications of current and future policies aimed at decarbonizing the shipping industry. It is highlighted that alternative zero-carbon fuels seem to be as the best path forward, while technological and operational changes alone won't fully decarbonize the industry, necessitating market-based measures. This study also highlights that some stakeholders will benefit more than others in the transition to a low-carbon shipping industry.

Christodoulou et al.[8] examines the economic effects of integrating the maritime sector into the EU emission trading system (EU-ETS). Using monitoring, reporting, and verification (MRV) data to assess CO_2 emissions within the European Economic Area (EEA), the study employs a scenario-based model considering factors like price incentives, geographical scope, and emission allowance distribution. The results indicate that a uniform benchmark for emission allowances would unfairly burden certain segments, particularly RoRo and RoPax vessels, due to their higher fuel consumption. To ensure fairness and encourage energy-efficient ships, the paper suggests the implementation of different benchmarks for each segment to avoid market distortions.
In this study, the application of heat recovery technology to a marine gas turbine was studied, however, the application of such technologies can be carried out in both industrial and marine applications.

Jouhara et al. [9] provides a comprehensive review of waste heat recovery technologies used in industrial processes to harness unused energy and reduce overall consumption. It examines recovery methods used in industries like steel, food, and ceramics, focusing on technologies such as recuperators, regenerators, heat exchangers, boilers, and heat pumps. Advanced techniques like membrane condensation, Organic Rankine cycles, and emerging technologies like thermoelectric and thermo-photovoltaic systems are also discussed. The study evaluates the advantages and drawbacks of each approach for converting waste heat into usable energy.

Baldi et al.[10] outlines a methodology for assessing the feasibility of installing a waste heat recovery (WHR) system on ships. It calculates the energy and exergy available from waste heat and compares it to the vessel's power needs, using exergy efficiency as a key variable. This approach helps estimate fuel savings without needing a detailed system design. Applied to a case study vessel, the method suggests potential fuel savings of 5%–15%, depending on the waste heat sources and system efficiency.

Singh et al.[11] provides an overview of the primary waste heat recovery (WHR) technologies used in marine applications. It examines systems such as the Rankine cycle, organic Rankine cycle, supercritical Rankine cycle, Kalina cycle, exhaust gas turbine systems, and thermoelectric generators. This study offers a comprehensive review of how these technologies utilize waste heat sources on marine vessels.

Suarez de la Fuente et al.[12] compares the performance of water and four organic fluids in waste heat recovery system across various engine operating conditions. It utilizes a representative ship operating profile and a typical marine generator to assess CO_2 emission reductions. Additionally, this paper discusses the risks associated with carrying flammable organic fluids on board. The findings indicate that a simple organic Rankine cycle can outperform a steam cycle under the same operating conditions.

The use of COGES systems has been considered as a solution to enable gas turbines to increase their efficiency to comparable levels with electric engines and to expand their use on commercial ships. Budiyanto et al.[13] assesses the techno-economic and environmental viability of the combined gas turbine and steam turbine integrated electric drive system (COGES) for liquefied natural gas (LNG) carriers. Evaluating a design for a 7500 m^3 LNG carrier, the study finds the system produces 1832 kilowatts at 12 knots with an efficiency of 30.1%. Economically, the COGES system shows a positive net present value, an internal rate of return of 12-18%, and a payback period of 6 to 8 years, indicating its potential as a viable, low-carbon propulsion technology.

Dotto et al.[14] examines the feasibility of Combined Gas Electric and Steam (COGES) systems on LNG vessels using a flexible tool. In this study is simulated the performance of six gas turbines and compares six integrated COGES-reciprocating engine power plants for cogeneration efficiency in the cruise-ferry GNV La Suprema. The results indicate that COGES systems are more efficient than reciprocating engines at the ship's cruising speed of 22 knots, with a 1–5% improvement in efficiency. COGES plants utilizing LM2500 and TITAN250 gas turbines achieve a maximum cogeneration efficiency of 51%.

In the present study, useful data for the individual parts of the marine COGES systems are initially listed. Subsequently, a thermodynamic analysis and heat transfer analysis is carried out for the heat recovery steam generator (HRSG). Next, a correlation is presented for the calculation of the total heat convection coefficient at partial loads for the HRSG. Then the modeling of the combined system in software is analyzed and the results of the parametric analysis of the COGES system for several fuels in a full range of loads are listed. Subsequently, a case study is carried out using COGES on a cruise ship for one year of operation in order to illustrate the improvement of the efficiency and the overall reduction of carbon dioxide emissions. It is worth noting that the case study is carried out for various combinations of alternative and conventional fuels.

2. Marine COGES Systems

Nowadays, ships have to conform to the strictest regulations imposed on international shipping. Also, shipping companies are trying to further reduce their operating costs, in which the cost of fuel occupies a dominant position. In order to be able to satisfy the two above requirements, the manufacturing companies try to continuously increase the efficiency of the propulsion vessel and, by extension, to reduce fuel consumption and pollutant emissions. A constantly developing technology is the combined systems, which consist of two different engineering systems, which are in interaction with each other. One category of these is the COGES Systems, which are examined in this study and will be analyzed in more detail below. These combined systems have so far been used on cruise ships (according to General Electric 8 ships used them until 2018) while in 2016 the classification society ABS approved the utilization of a dual fuel COGES system for the construction of an LNG ship.

2.1 COGES Systems

COGES systems consist of a gas turbine, which is used to propel the ship, and a steam turbine, which uses the large amounts of heat in the exhaust gases to generate electricity. The steam cycle usually uses water as working mean and is based thermodynamically on the Rankine cycle. In the international literature, these systems show a high efficiency of around 50% [15], [16], [17]. The use of the steam turbine is particularly important in these systems as the exhaust gases exit the gas turbine at particularly high temperatures of 450-600 C and contain particularly large amounts of waste heat [18]. An important issue arising from the use of this system is the types of fuel that can be used for combustion as the fuel plays a significant role in the overall cost of the investment and it will be analyzed further in Chapter 2.3. As far as the economic feasibility is concerned, Ahn et al [19] examined that the utilization of proper fuel in this system can make this investment highly promising. Another important aspect is the environmental footprint of this system in comparison to the existing propulsion systems. Several studies have shown that this technology can be a solution to the growing restrictions for the gaseous emissions [20]. Ahn et al. stated that this system can make a ship be compliant with the Phase 2 and 3 of EEDI and even with the Phase 4 if it is imposed in the near future, being a solution to a significant trouble of shipping businesses. This is because gas turbines use more environmentally friendly fuels and the overall thermal efficiency of the system is kept on high levels. Another advantage of this system is its low maintenance cost, its high reliability and the necessity for fewer crew members [21].

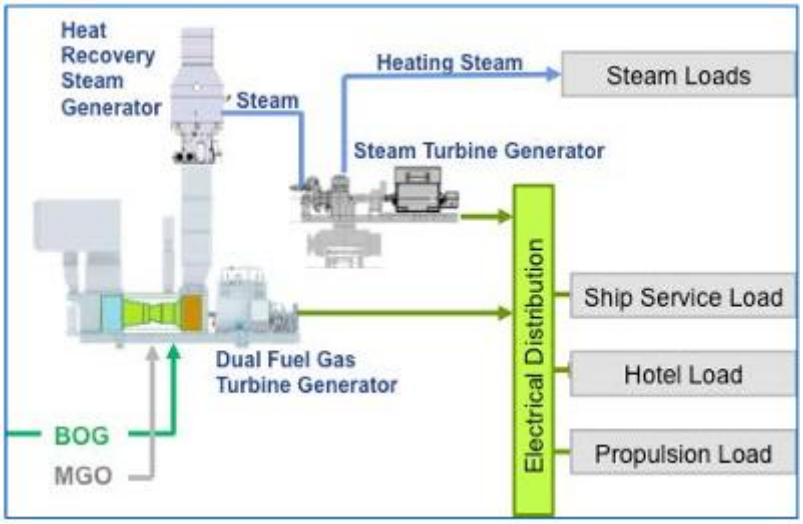

Figure 1. COGES System-Schematic Illustration

2.2 Gas Turbines-Fuels

Gas Turbines are mainly used in airplanes but with some modifications are capable of being used in maritime applications (aero derivative gas turbine). The marine gas turbines are a widely known way of propulsion for warships and cruise ships and generally in applications where the ship need to adapt quickly different speeds. As the name suggests, aero-derivative gas turbines are evolved from turbofan engines used in aircraft. The gas generator and the free power turbine are the two main components of the gas turbine. Without the large fan up front, the gas generator is the jet engine's central component. On the gas generator's exhaust side is where the free power turbine is installed. Its goal is to transform the energy found in the exhaust gas stream into a rotating action that can power a generator, a waterjet, or a propeller. The phrase "free power turbine" denotes that there is no physical connection between the shafts of the gas generator and the free power turbine. Through the gas generator's exhaust gases exiting, they are connected aerodynamically. Special coatings are applied to the gas generator's compressor blades in maritime applications to increase their resistance to the effects of the salt in the intake air. Armellini et al. [22] discussed the concern over NOx and SOx emissions from merchant ships, the stricter IMO regulations, and evaluated the use of Gas Turbines fueled by MGO as a potential solution to meet the new regulations, providing a detailed quantification of the differences in weight, room, fuel consumption, and pollutant emissions for different engine configurations. Sayma [23] stated that gas turbines have been established for naval and high-speed civilian ships, but their use in merchant ships is limited due to factors like efficiency and fuel costs. This paper analyzed the advantages and limitations of gas turbines, as well as potential future developments in the field. Barsi [24] evaluated Mini Gas Turbine Cycles for heat and power generation on commercial vessels, highlighting their competitive cogeneration performance compared to commercial Gas Turbines and Marine Diesel engines. An evolution of the gas turbine is combined gas turbine and steam turbine, which are capable of achieving high levels of thermal efficiency and meeting the stricter requirements for gaseous emissions. Dotto et al. [25] stated that COGES systems are able to achieve high thermal efficiency(47-52%) and meet the EEDI requirements for the period after 2025. Budiyanto et al. [13] examined the feasibility of an investigation of this system for a LNG carrier and concluded that a payback period of almost 8 years is required.

A range of studies have explored the use of alternative fuels in gas turbines, with a focus on reducing emissions and increasing efficiency. Larfeldt [26] and Moliere [27] discussed the

versatility of gas turbines in terms of fuel options, their low emissions compared to coal-fired plants, the potential for further reducing CO_2 emissions with carbon capture and storage technology, and the challenges associated with handling different fuels and ensuring proper combustion. Welch et al [28] studied various types of gaseous and liquid fuels that can be utilized in gas turbines and highlights the impact of common contaminants found in fuels on the operability and maintenance of gas turbines. Stefanizzi [29] and Enagi et al [30] discussed the use of biofuels in clean combustion methods for gas turbines to achieve ultra-low emissions of NOx and CO, and proposed further research to enhance the versatility of liquid biofuels in gas turbines. Ghenai [31] mentioned the historical use of methane fuel, the shift towards hydrogen-rich fuels with IGCC technology, fuel flexibility issues, lean premixed combustion for low NOx emissions, and challenges posed by hydrogen enrichment on flame behavior.

Once-Through Boiler

A significant feature of the COGES system is its main heat exchanger where the exhaust gas transfer heat to the feed water, which is the working mean of the system. Several types of heat exchangers have been examined in waste heat recovery systems but in this study an once-through steam generator is examined. This type of heat exchanger is a key component in combined cycle applications, which has been the subject of extensive research. Dechamps [32] highlighted its potential for high-pressure and supercritical steam conditions. Naess [33] conducted a parametric analysis of geometrical characteristics for the evaluation of heat transfer coefficient and pressure drop of a once-through heat exchanger.

Methodology

The main objective of this study is to model the combined gas turbine and heat recovery system. The initial step is the modeling of the once-through steam generator with the aim of calculating the overall heat transfer coefficient at full and partial loads. At the same time, the effect of the change in the geometrical characteristics of the exchanger on the change in the value of the overall heat transfer coefficient is illustrated diagrammatically. Then the least squares method is applied with the aim of deriving a correlation of the overall heat transfer coefficient as a function of mass supply and exhaust gas temperature at some loads. These data are then entered into a thermal system simulation program. Afterwards, optimization of the operating parameters of the system is performed in the simulation program with the aim of maximizing its power output and thermal efficiency. The operating parameters that are studied are the high pressure and the superheating degree of the system. The optimization is performed separately for several fuels and in a load range of 50-100%. Afterwards, a correlation is created which will calculate the optimal conditions at partial loads as a function of mass supply and exhaust temperature at partial loads. Finally, the power generation from the heat recovery system as well as the overall thermal efficiency of the combined system is calculated and represented diagrammatically.

3. HRSG Analysis

3.1 System Description

The examined waste heat recovery system is based on the Organic Rankine Cycle principals. It exploits the rejected thermal energy of the exhaust gas of a gas turbine utilizing water as working mean. In this system the feed water enters the feedwater pumps in order to obtain high pressure. Subsequently, it enters the Preheater, where is preheated and after this process a small portion of the stream is isolated and enters two flash separators. Afterwards, the stream enters successively the Evaporator and the Superheater and exits as superheated stream. Then, the stream is expanded in the turbine producing electricity in the clutched generator. The expanded working mean exits the Expander and enters the condenser in order to be saturated liquid. This mixture enters the two condensate pumps and is driven into the condensate polishing plant so as to repeat the thermodynamic cycle.

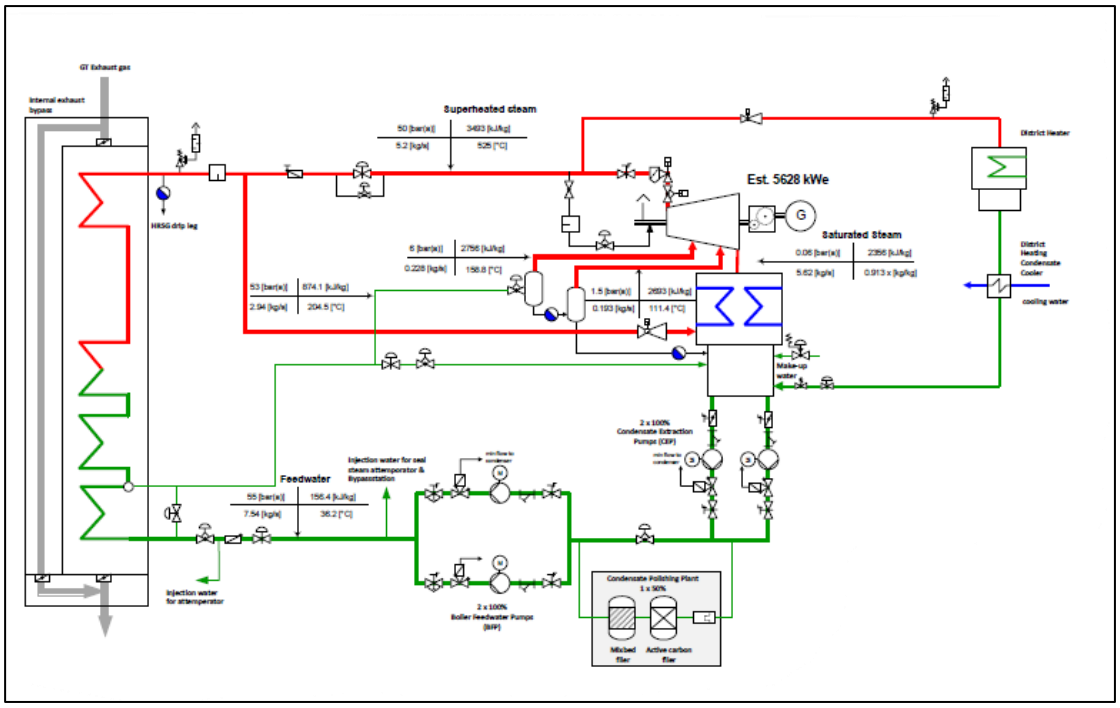

Figure 2. Schematic Diagram of the System

3.2 Thermodynamic Analysis

1.1 State 1 – State 2: Condensation Extraction Pumps

The power consumed by the condensation pumps is:

$$\dot{W}_{cond,pump} = \dot{m}_{water}\left(h_{ST2} - h_{ST1}\right) \quad (1)$$

The isentropic efficiency of the condensation pumps is:

$$n_{CondPump,is} = \frac{h_{ST2is} - h_{ST1}}{h_{ST2} - h_{ST1}} \tag{2}$$

1.2 State 2 – State 3: Boil Feedwater Pumps

The power consumed by the boil feedwater pumps is:

$$\dot{W}_{feed,pump} = \dot{m}_{water}\left(h_{ST3} - h_{ST2}\right) \tag{3}$$

The isentropic efficiency of the boil feedwater pumps is:

$$n_{FeedPump,is} = \frac{h_{ST3is} - h_{ST2}}{h_{ST3} - h_{ST2}} \tag{4}$$

1.3 State 3 – State 4 – State 5: Preheater

The transferred heat from the exhaust gas in the Preheater before the removal part of the mass flow rate is:

$$\dot{Q}_{Preheater,bef} = \dot{m}_{water}\left(h_{ST4} - h_{ST3}\right) = \varepsilon_{Preheater,bef} \cdot \dot{m}_{exh,gas}\left(h_{gas1} - h_{gas2}\right) \tag{5}$$

The percentage of the removed mass flow rate of the working mean is:

$$a_{Preheater} = \frac{\dot{m}_{water,rem}}{\dot{m}_{water}} \tag{6}$$

The evaluation of area of this heat exchanger is based on the logarithmic mean temperature difference (LMTD). Based on this method, the heat transfer rate is also calculated as follows:

$$\dot{Q}_{Preheater,bef} = U_{Preheater,bef} A_{Preheater,bef} \Delta T_{LMTD,Pre,bef} \tag{7}$$

where $\Delta T_{LMTD} = \frac{\Delta t_{max} - \Delta t_{min}}{ln\frac{\Delta t_{max}}{\Delta t_{min}}}$, $\Delta t_{max} = T_{gas,1} - T_{ST7}$ and $\Delta t_{min} = T_{gas,5} - T_{ST3}$

The remaining percentage receives heat from the exhaust gas as follows:

$$\dot{Q}_{Preheater,aft} = (1 - a_{Preheater}) \cdot \dot{m}_{water} \left(h_{ST5} - h_{ST4} \right) = \varepsilon_{Preheater} \cdot \dot{m}_{exh,gas} \left(h_{gas2} - h_{gas3} \right) \quad (8)$$

$$\dot{Q}_{Preheater,aft} = U_{Preheater,aft} A_{Preheater,aft} \Delta T_{LMTD,Pre,aft} \quad (9)$$

1.4 State 5 – State 6: Evaporator

The transferred heat from the exhaust gas in the Evaporator is calculated as follows:

$$\dot{Q}_{Evaporator} = (1 - a_{Preheater}) \dot{m}_{water} \left(h_{ST6} - h_{ST5} \right) = \varepsilon_{Evaporator} \cdot \dot{m}_{exh,gas} \left(h_{gas3} - h_{gas4} \right) \quad (10)$$

$$\dot{Q}_{Evaporator} = U_{Evaporator} A_{Evaporator} \Delta T_{LMTD,Evaporator} \quad (11)$$

1.5 State 6 – State 7: Superheater

The transferred heat from the exhaust gas in the Superheater is:

$$\dot{Q}_{Superheater} = (1 - a_{Preheater}) \dot{m}_{water} \left(h_{ST7} - h_{ST6} \right) = \varepsilon_{Superheater} \cdot \dot{m}_{exh,gas} \left(h_{gas4} - h_{gas5} \right) \quad (12)$$

$$\dot{Q}_{Superheater} = U_{Superheater} A_{Superheater} \Delta T_{LMTD,Super} \quad (13)$$

1.6 State 7 – State 8 – State 9- Stage 10: Multi-Stage Turbine

The power generated by the turbine in a multi-stage process is calculates by the following equations. The superheated stream is expanded partially until the first intermediate pressure as follows:

$$\dot{W}_{exp1} = (1 - a_{Preheater})\dot{m}_{Water}\left(h_{ST7} - h_{ST8}\right) \tag{14}$$

The isentropic efficiency of the first expansion process is:

$$n_{Turbine1,is} = \frac{h_{ST7} - h_{ST8}}{h_{ST7} - h_{ST8is}} \tag{15}$$

Then the stream is mixed with the stream which exits the first flash separator as follows:

$$(1 - a_{Preheater} + a_{flash,1})\dot{m}_{Water}h_{ST8'} = (1 - a_{Preheater})\dot{m}_{Water}h_{ST8} + a_{flash,1}\dot{m}_{Water}h_{flash,1} \tag{16}$$

where $a_{flash,1} = \frac{\dot{m}_{water,flash,1}}{\dot{m}_{water}}$ which is the mass flow rate that exits the first flash separator divided by the whole mass flow rate.

Afterwards, the mixed proportion of stream is expanded again in the turbine until the second intermediate pressure as shown below:

$$\dot{W}_{exp2} = (1 - a_{Preheater} + a_{flash,1})\dot{m}_{Water}\left(h_{ST8'} - h_{ST9}\right) \tag{17}$$

The isentropic efficiency of the second expansion process is:

$$n_{Turbine2,is} = \frac{h_{ST8} - h_{ST9'}}{h_{ST8} - h_{ST9'is}} \tag{18}$$

Subsequently, the stream at State 9 is mixed again with the stream, which exits the second flash separator, as it is illustrated in the following equation:

$$(1 - a_{Preheater} + a_{flash,1} + a_{flash,2})\dot{m}_{Water}h_{ST9'} = (1 - a_{Preheater} + a_{flash,1})\dot{m}_{Water}h_{ST9} + a_{flash,2}\dot{m}_{Water}h_{flash,2} \tag{19}$$

where $a_{flash,2} = \frac{\dot{m}_{water,flash,2}}{\dot{m}_{water}}$ which is the mass flow rate that exits the second flash separator divided by the whole mass flow rate.

The final mass flow rate is expanded until the lowest pressure of the cycle. The equations of this process are depicted below:

$$\dot{W}_{exp3} = (1 - a_{Preheater} + a_{flash,1} + a_{flash,2})\dot{m}_{Water}\left(h_{ST9'} - h_{ST10}\right) \quad (20)$$

The isentropic efficiency of the third expansion process is:

$$n_{Turbine3,is} = \frac{h_{ST9'} - h_{ST10}}{h_{ST9'} - h_{ST10is}} \quad (21)$$

1.7 State 10- Stage 1: Condenser

In the condenser rejects heat to the organic medium of the LT loop:

$$\dot{Q}_{Condenser} = \varepsilon_{Cond} \cdot \dot{m}_{Water}\left(h_{ST10} - h_{ST1}\right) = \dot{m}_{CWater}\left(h_{CWater,out} - h_{CWater,in}\right) \quad (22)$$

$$\dot{Q}_{Condenser} = U_{Condenser} A_{Condenser} \Delta T_{LMTD} \quad (23)$$

The net power output of the cycle is:

$$\dot{W}_{net} = \dot{W}_{exp,1} + \dot{W}_{exp,2} + \dot{W}_{exp,3} - \dot{W}_{cond,pump} - \dot{W}_{feed,pump} \quad (24)$$

3.3 Heat Transfer Analysis

The overall heat transfer coefficient is calculated as follows:

$$\frac{1}{U} = \frac{1}{h_{in}} + FF_{in} + FF_{out} + \frac{1}{h_{out}} + \frac{t_w}{\lambda} \tag{25}$$

where FF is the fouling factor, t_w is the thickness of the tube, λ the thermal conductivity of the material of the tube and h the heat transfer coefficient of the internal and external flow.

3.3.1 External Heat Transfer Coefficient

The external heat transfer coefficient is given by the following relation:

$$h_{out} = \frac{Nu_{gas} \cdot \lambda_{gas}}{d_o} \tag{26}$$

where the Nusselt Number is described by the following relations [33]:

$$Nu_{gas} = 0.107 \cdot Re_{gas}^{0.65} \cdot Pr_{gas}^{1/3} \cdot \left(\frac{P_t}{d_e}\right)^{0.35} \cdot \left(\frac{l_e}{d_e}\right)^{-0.13} \cdot \left(\frac{l_e}{s_f}\right)^{-0.14} \cdot \left(\frac{s_f}{d_e}\right)^{-0.2} \text{ for } S_t/S_d<1 \tag{27}$$

$$Nu_{gas} = 0.141 \cdot Re_{gas}^{0.65} \cdot Pr_{gas}^{1/3} \cdot \left(0.43 + 9.75 \cdot e^{-3.23 \cdot (S_t/S_d)}\right) \cdot \left(\frac{l_e}{d_e}\right)^{-0.13} \cdot \left(\frac{l_e}{s_f}\right)^{-0.14} \cdot \left(\frac{s_f}{d_e}\right)^{-0.2} \text{ for } S_t/S_d>1 \tag{28}$$

where P_t is the transverse tube pinch, d_e effective tube outer diameter, l_e net fin height ($h_f - t_f$), t_f fin thickness and s_f is fin pinch.

$$Re_{gas} = \frac{D_e \cdot W_c}{a_s \cdot \mu} \text{ (Reynolds Number)} \tag{29}$$

where a_s is the flow area, W_c is the gas flow, μ is the viscosity and D_e is the equivalent diameter.

$$a_s = W \cdot L - n_{tf} \cdot L \cdot \left[D_o + n_f \cdot h_f \cdot t_f \right] \text{(Flow Area)} \tag{30}$$

where n_{tf} is the number of tubes per row, h_f is the height of the fin, n_f is the number of fins per meter of tube.

$$De = \frac{2 \cdot (A_F + A_D)}{\pi \cdot (projected\_diameter)} \text{ (Equivalent Number)} \tag{31}$$

$$A_D = \pi \cdot d_o (1 - t_f \cdot n_f) \tag{32}$$

$$A_F = \pi \cdot 2 \cdot n_f \cdot \left[\left(h_f + d_o \right)^2 - d_o^2 \right] / 4 \tag{33}$$

$$projected\_diameter = 2 \cdot h_f \cdot n_f + 2 \cdot (1 - t_f \cdot n_f) \tag{34}$$

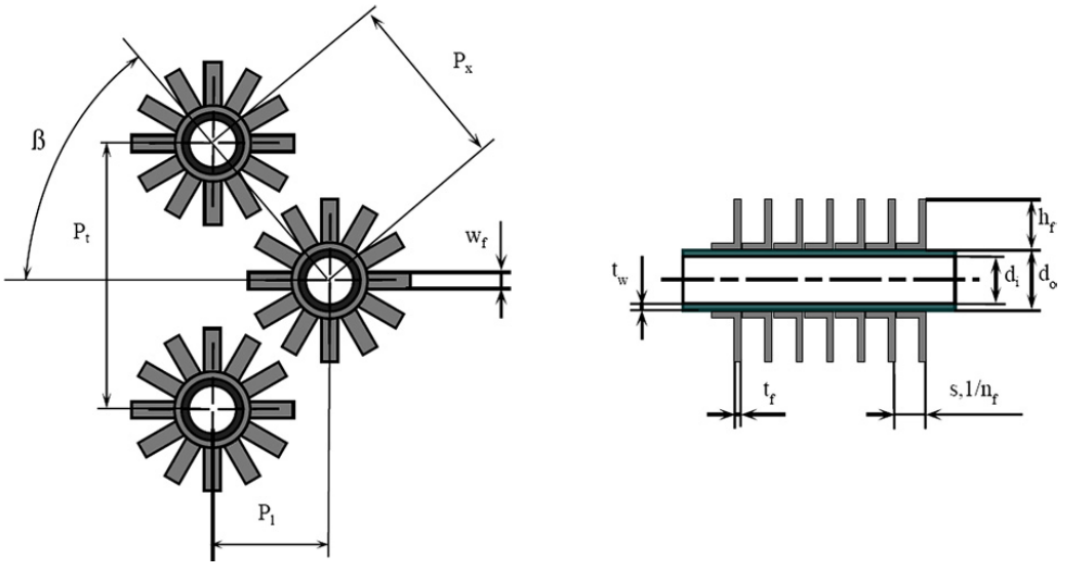

Figure 3. Geometrical Parameters of the Once-Through Boiler

3.3.2 Internal Heat Transfer Coefficient

The internal heat transfer coefficient is given by the following relation:

$$h_{in} = \frac{Nu_{water} \cdot \lambda_{in}}{d_{in}} \tag{35}$$

where the Nusselt Number is described by the following correlation of Gnielinski [34]:

$$Nu_{water} = \frac{\left(f/8\right) \cdot \left(Re_{water} - 1000\right) \cdot Pr}{1 + 12.7 \cdot \left(f/8\right)^{0.5} \cdot \left(Pr^{2/3} - 1\right)} \cdot \left[1 + \left(\frac{D_h}{L}\right)^{2/3}\right] \cdot \left(\frac{Pr}{Pr_w}\right)^{0.11} \tag{36}$$

where f is the friction number with the relation below:

$$f = \left(1.82 \cdot \log\left(\mathrm{Re}_{water}\right) - 1.64\right)^{-2} \tag{37}$$

the Reynolds Number is calculated as follows:

$$Re_{water} = \frac{D_h \cdot \rho_{water}}{\mu_{water}} \tag{38}$$

the ratio $\frac{\mathrm{Pr}}{\mathrm{Pr}_w} \sim 0.05 - 20$ according to Cao [35] and D_h is the hydraulic diameter of the tube.

3.3.3 Geometrical Characteristics of the Once-Through Heat Exchanger

The geometrical characteristics of the heat exchanger plays an important role in the value of the external heat transfer coefficient and for this reason their effect will be investigated in a range of values in the calculation of the value of the external heat transfer coefficient. Some of the characteristics of the heat exchanger were obtained from the data provided by the manufacturer while some others were studied in a range of values, which were taken from the international literature.

Table 1. Constant and Variable Parameters of the Heat Exchanger

Heat Exchanger Data	**Constant Parameters**	**Outer Diameter(m)**	0.0254
		Internal Diameter(m)	0.0191
		External Diameter with Fin Thickness(m)	0.0318
		Number of Rows	30
		Number of Tubes per Row	36
		W(m)	3.18
		L_{eff}(m)	5
	Variable Parameters		**Range**
		Number of Fins per Meter	275-433
		Fin Height(m)	0.008-0.0105
		Transverse Tube Pinch P_t(m)	0.065-0.09

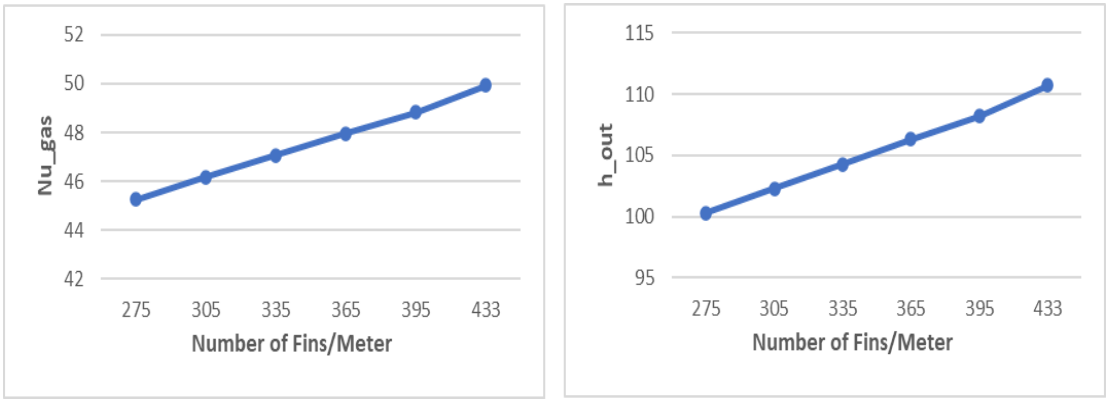

Figure 4. Alteration of Nusselt Number and of the external heat transfer coefficient depending on the Number of Fins

In Figure 4 is depicted the impact of the number of fins in the value of Nusselt Number and the external heat transfer coefficient with this number ranging from 275 to 433. As the number of fins is increased, both of the examined parameters are increased with the difference between the lowest and the highest price of them being approximately 10%.

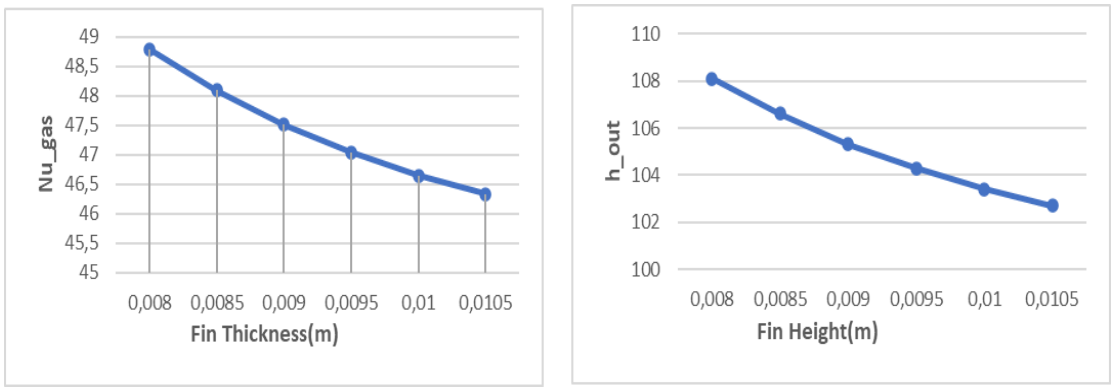

Figure 5. Alteration of Nusselt Number and of the external heat transfer coefficient depending on the Fin Thickness

In Figure 5 is illustrated the impact of the fin thickness in the value of Nusselt Number and the external heat transfer coefficient with the thickness ranging from 0.008 mm to 0.0105 mm. As the fin thickness is increased, both of the examined parameters are decreased with the difference between the lowest and the highest price of them being approximately 6%.

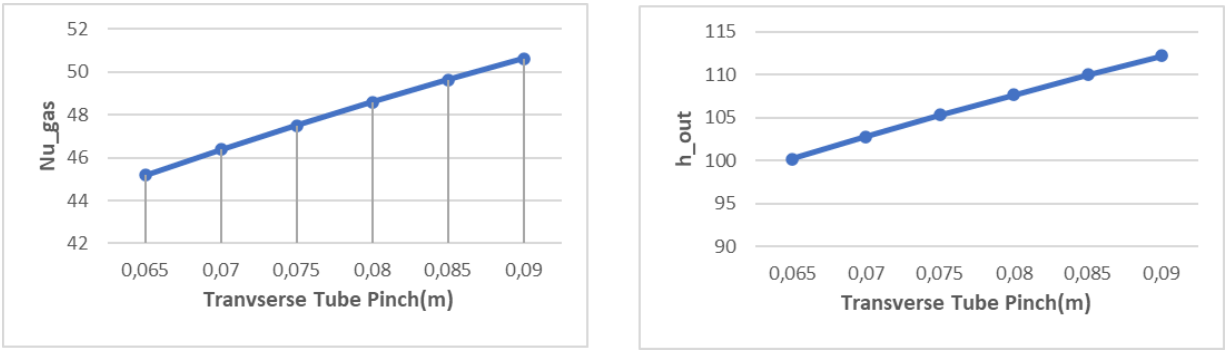

Figure 6. Alteration of Nusselt Number and of the external heat transfer coefficient depending on the Transverse Tube Pinch

In Figure 6 is shown how does the transverse tube pinch affect the value of Nusselt Number and the value of the external heat transfer coefficient with the pinch ranging from 0.065 m to 0.09 m. As the tube pinch gets higher values, both of the examined parameters are increased with the difference between the lowest and the highest price of them being approximately 12%. For the final values of the examined parameters were considered the average terms of the studied range.

3.3.4 Calculation of the Overall Heat Transfer Coefficient

The overall heat transfer coefficient, as it is referred in Chapter 3.3 by the equation 25, is dependent to the inner and the outer heat transfer coefficient, to the heat transfer coefficient of the heat exchanger and to the inner and outer fouling factor. If it assumed that the heat exchanger is in good condition and the fouling factor is neglected. Furthermore, the factor of the heat exchanger can also be neglected due to its low affection. Consequently, the relation is simplified as follows:

$$\frac{1}{U} = \frac{1}{h_{in}} + \frac{1}{h_{out}} \tag{39}$$

In the international literature, most researches consider that the overall heat transfer coefficient in once-through heat exchangers is equivalent to the external heat transfer coefficient and consider that the effect of the internal heat transfer coefficient is negligible. This assumption in the context of this research will be checked in order to see how it is correct in our case and in order to carry out the necessary simplifications if they are needed in order to proceed with calculations. These calculations were carried out in the computational program EES, in which initially the energy analysis of the system was conducted and then the heat transfer analysis took place in order to determine the heat transfer coefficients values. In order to make the energy and heat transfer analysis, performance data from the manufacturer of this system was used. The results from the heat transfer analysis are illustrated below:

Table 2. Calculation of the heat transfer coefficients in the initial part of the Preheater

Preheater$_1$				
Load	**h_out**	**h_in**	**U**	**deviation h_out-U**
100%	91.17	7234	90.04	1.260%
90%	88.86	6802	87.71	1.306%
80%	86.04	6403	84.90	1.344%
70%	83.1	6239	82.01	1.332%
60%	80.19	6076	79.15	1.320%
50%	77.25	5856	76.24	1.319%

Table 3. Calculation of the heat transfer coefficients in the final part of the Preheater

Preheater$_2$				
Load	**h_out**	**h_in**	**U**	**deviation h_out-U**
100%	97.13	6345	95.67	1.531%
90%	94.36	5951	92.89	1.586%
80%	91.13	5590	89.67	1.630%
70%	88.09	5449	86.69	1.617%
60%	85.09	5317	83.75	1.600%
50%	82	5126	80.71	1.600%

Table 4. Calculation of the heat transfer coefficients in the Evaporator

Evaporator				
Load	**h_out**	**h_in**	**U**	**deviation h_out-U**
100%	104.5	90387	104.38	0.116%
90%	101.3	88812	101.18	0.114%
80%	97.79	88446	97.68	0.111%
70%	94.72	88340	94.62	0.107%
60%	91.71	88299	91.61	0.104%
50%	88.51	87561	88.42	0.101%

Table 5. Calculation of the heat transfer coefficients in the Superheater

Superheater				
Load	**h_out**	**h_in**	**U**	**deviation h_out-U**
100%	112.2	2639	107.62	4.252%
90%	108.6	2421	103.94	4.486%
80%	104.8	2222	100.08	4.716%
70%	101.7	2160	97.13	4.708%
60%	98.63	2103	94.21	4.690%
50%	95.29	2020	91.00	4.717%

From the above tables. can be easily notified that the external heat convection coefficient differs from the internal heat input coefficient in a very small percentage. Specifically in the preheater, the difference is of the order of 1.5%, in the vaporizer, the difference is of the order of 0.1% while the biggest difference is found in the superheater where the difference is around 4.5%. the above comparison can easily make us find that the external heat convection coefficient can describe with great accuracy the total heat convection coefficient therefore and based on what is presented in the international literature. it will be considered in this paper that the affection of the internal heat transfer coefficient is negligible, so it will not be taken into consideration. This assumption as it turned out and from the calculations. it will not lead to a big error in the calculations.

$$U \simeq h_{out} \tag{40}$$

3.4 Heat Transfer Analysis Correlation-Validation

After the heat transfer analysis. a correlation was created in order to directly calculate the total heat convection coefficient at partial loads without requiring a reanalysis. In particular. it is required to carry out the analysis at 100% of the engine load and then using the mass supply and the temperature of the exhaust gases at their exit from the engine through the correlation. The calculation of the total heat convection coefficient was carried out at the EES. The form of the correlation of the total heat transfer coefficient is listed below:

$$U_{correlation} = U_{100\%-calculated} \cdot \left(\frac{m_{gas-PartialLoad}}{m_{gas-100\%}} \right)^{x} \cdot \left(\frac{T_{gas-PartialLoad}}{T_{gas-100\%}} \right)^{y} \tag{41}$$

Then using the calculating program Excel, it was inserted the equation of MAPE, which is the sum of the deviation between the calculated and the predicted overall heat transfer coefficient in the part loads of 50-90% for all the units of the once-through boiler as illustrated below. The MAPE was minimized using the Solver of the referred program.

$$MAPE(x,y) = \frac{\sum_{Units} \sum_{50\%}^{90\%} \frac{U_{correlation}(x,y) - U_{calculated}}{U_{calculated}}}{\sum Units \cdot \sum Loads} \tag{42}$$

The solution of the equation is the following:

$$\min(MAPE) \rightarrow x = 0.663,\ y = 0.168 \tag{43}$$

The final version of the correlation is the equation below:

$$U_{correlation} = U_{100\%-calculated} \cdot \left(\frac{m_{gas-PartialLoad}}{m_{gas-100\%}} \right)^{0.663} \cdot \left(\frac{T_{gas-PartialLoad}}{T_{gas-100\%}} \right)^{0.168} \tag{44}$$

The results presented below show the high accuracy of the correlation approach. In all sections of the exchanger the deviation is less than 0.5% in relation to the results of the calculated heat transfer analysis.

Table 6. Comparison between the calculated U and the U of the correlation in the Superheater

	Superheater		
Load(%)	**$U_{calculated}$**	**$U_{correlation}$**	**deviation**
100	72.880	72.880	
90	70.550	70.549	0.001%
80	68.030	68.042	0.017%
70	66.020	66.020	0.000%
60	64.040	64.049	0.014%
50	61.880	61.880	0.000%
	mean deviation		0.006%

Table 7. Comparison between the calculated U and the U of the correlation in the Evaporator

Evaporator			
Load(%)	**$U_{calculated}$**	**$U_{correlation}$**	**deviation**
100	67.890	67.890	
90	65.810	65.852	0.063%
80	63.500	63.615	0.181%
70	61.510	61.659	0.243%
60	59.550	59.756	0.346%
50	57.480	57.691	0.367%
	mean deviation		0.240%

Table 8. Comparison between the calculated U and the U of the correlation in the initial part of the Preheater

$Preheater_1$			
Load(%)	**$U_{calculated}$**	**$U_{correlation}$**	**deviation**
100	59.200	59.200	
90	57.700	57.462	0.101%
80	55.870	55.462	0.139%
70	53.960	53.646	0.083%
60	52.070	51.864	0.011%
50	50.160	49.999	0.032%
	mean deviation		0.073%

Table 9. Comparison between the calculated U and the U of the correlation in the final part of the Preheater

Preheater$_2$			
Load(%)	**$U_{calculated}$**	**$U_{correlation}$**	**deviation**
100	63.070	63.070	
90	61.280	61.387	0.139%
80	59.170	59.392	0.219%
70	57.200	57.399	0.155%
60	55.260	55.439	0.062%
50	53.250	53.404	0.066%
	mean deviation		0.128%

The mean deviation from all the units of the once-through boiler and for the part loads between 50-90% is 0.178%, which depicts the high accuracy of the produced equation.

4. Modelling of the Combined System

The combined system was modeled in the Siemens gPROMS® Advanced Process Modelling® platform. gPROMS (general PROcess Modelling System) is a powerful process modelling and simulation software widely used in the energy, chemical and pharmaceuticals industries. It allows to develop, simulate, and optimize complex dynamic process models, capturing their behaviour across various dynamic and steady-state conditions. A key feature of gPROMS is its equation-oriented approach, where process models are formulated as systems of equations, very similar to the actual mathematical formulation. The platform was utilized in order to combine the 3 main parts of the considered system (the gas turbine. the once-through boiler and the steam turbine) and simulate their operation. As it was mentioned above. the exhaust gases exit the gas turbine and then enter the central exchanger where they heat feed water. which is then expanded in the steam turbine producing electricity in a generator. The way to model each part of the installation will be extensively analyzed and an overall picture of the simulated installation will be presented.

4.1 GT

The gas turbine that was studied in a specific study was the SGT-400, which was manufactured by Siemens for maritime applications. The Siemens SGT-400 is a mid-sized industrial gas turbine designed for power generation and mechanical drive applications. It offers a power output of around 10 to 15 megawatts (MW) and is known for its high efficiency, reliability. and low emissions. The turbine is designed with thermal efficiency of around 35-37% in simple cycle mode, which can be significantly higher in combined cycle configurations. This makes it a cost-effective choice for energy-intensive industries. The turbine features a compact, modular design that simplifies installation and maintenance and it can operate on a variety of fuels, including natural gas and liquid fuels. The SGT-400 is often used in combined heat and power (CHP) plants. industrial cogeneration. and in the oil and gas industry for driving compressors and pumps. For this particular gas turbine, performance maps were used for every operating part load as well as measurements at 100% of its operation for various types of fuels. The performance maps contain information about the produced power, the thermal efficiency, the exhaust gas outlet temperature and the exhaust gas mass supply as shown in the image below.

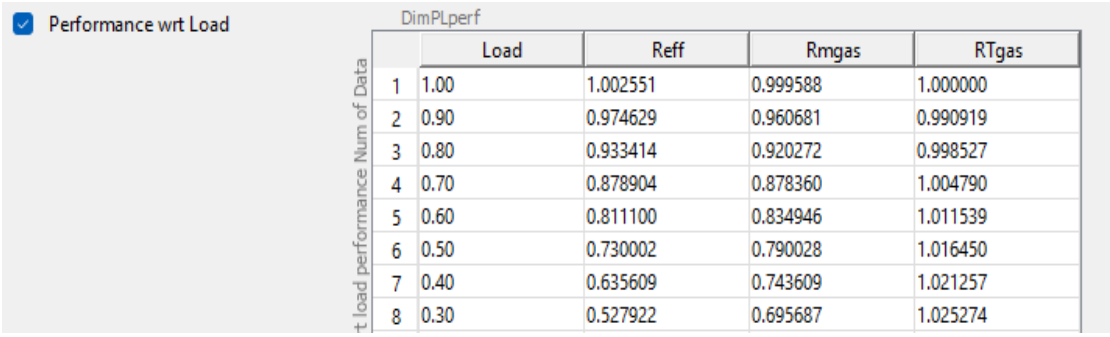

	Load	Reff	Rmgas	RTgas
1	1.00	1.002551	0.999588	1.000000
2	0.90	0.974629	0.960681	0.990919
3	0.80	0.933414	0.920272	0.998527
4	0.70	0.878904	0.878360	1.004790
5	0.60	0.811100	0.834946	1.011539
6	0.50	0.730002	0.790028	1.016450
7	0.40	0.635609	0.743609	1.021257
8	0.30	0.527922	0.695687	1.025274

Figure 6. Performance Maps of the Gas Turbine

In addition, measurements from the manufacturer were utilized for the 100% load of the gas turbine operation using different types of fuel and in different environmental conditions. In this case, the studied parameters were the produced power, thermal efficiency, exhaust gas mass flow and exhaust gas temperature as illustrated below:

Table 10. Measurement of operating parameters of the GT using Hydrogen

Fuel	Hydrogen			
Gearbox Output (kW)	12103	11482	10899	10351
Thermal Efficiency (LHV) (%)	35.13	34.59	34.03	33.47
Exhaust Flow (kg/s)	38.13	36.79	35.52	34.28
Exhaust Temp. (C)	525.5	532	538.7	545.5
Eng. Inlet Temp. (C)	10	15	20	25

Table 11. Measurement of operating parameters of the GT using LNG

Fuel	LNG			
Gearbox Output (kW)	10942	10361	9829	9353
Thermal Efficiency (LHV) (%)	33.74	33.17	32.62	32.06
Exhaust Flow (kg/s)	36.74	35.44	34.21	33.12
Exhaust Temp. (C)	536.6	543.3	550	556.6
Eng. Inlet Temp. (C)	10	15	20	25

Table 12. Measurement of operating parameters of the GT using a mixture 70% Hydrogen and 30% LNG as fuel

Fuel	70%H2-30%LNG			
Gearbox Output (kW)	11393	10796	10235	9736
Thermal Efficiency (LHV) (%)	34.3	33.75	33.19	32.64
Exhaust Flow (kg/s)	37.29	35.97	34.69	33.55
Exhaust Temp. (C)	532.1	538.7	545.5	552.1
Eng. Inlet Temp. (C)	10	15	20	25

Table 13. Measurement of operating parameters of the GT using a mixture 80% Hydrogen and 20% LNG as fuel

Fuel	80%H2-20%LNG			
Gearbox Output (kW)	11549	10949	10380	9871
Thermal Efficiency (LHV) (%)	34.5	33.95	33.38	32.82
Exhaust Flow (kg/s)	37.48	36.15	34.87	33.72
Exhaust Temp. (C)	530.6	537.1	543.9	550.6
Eng. Inlet Temp. (C)	10	15	20	25

Table 14. Measurement of operating parameters of the GT using Methanol

Fuel	Methanol	
Generator Output (kW)	10933	9351
Thermal Efficiency (LHV) (%)	33.27	31.62
Exhaust Flow (kg/s)	37.46	33.68
Exhaust Temp. (C)	530.3	550.3
Eng. Inlet Temp. (C)	15	30

Another important aspect of the GT modelling is the analysis of the fuel composition of each fuel, which is necessary to be imported in the program as shown below:

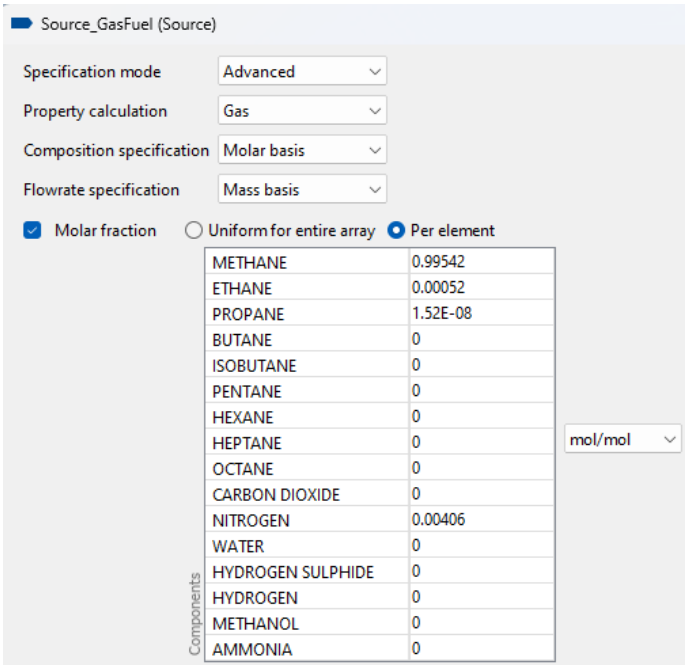

Figure 7. Insert of the fuel composition in the Gproms

4.2 Once-Through Boiler

The next component of the installation is the once-through boiler which was modelled in the Gproms. It is necessary to insert in the program the total heat transfer area, the mass flow rate of

the water and either the final temperature of the water or the superheating degree of the water on the exit of the heat exchanger as depicted in the following figure.

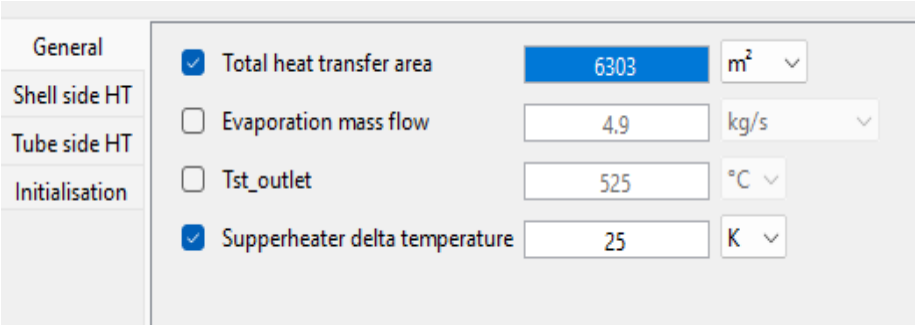

Figure 8. Insert of General Features of the Once-Through boiler

Afterwards, it is needed to insert a part load model in the analysis of the inside and outside part of the heat exchanger, but due to our assumption the inside heat transfer coefficient is negligible. As far as the outside part of the heat exchanger is concerned, the produced correlation will be used in order to fill the necessary cells in the program. As it is demonstrated in the next Figure, the heat transfer coefficient in full load and the factors of the correlation are inserted in the program.

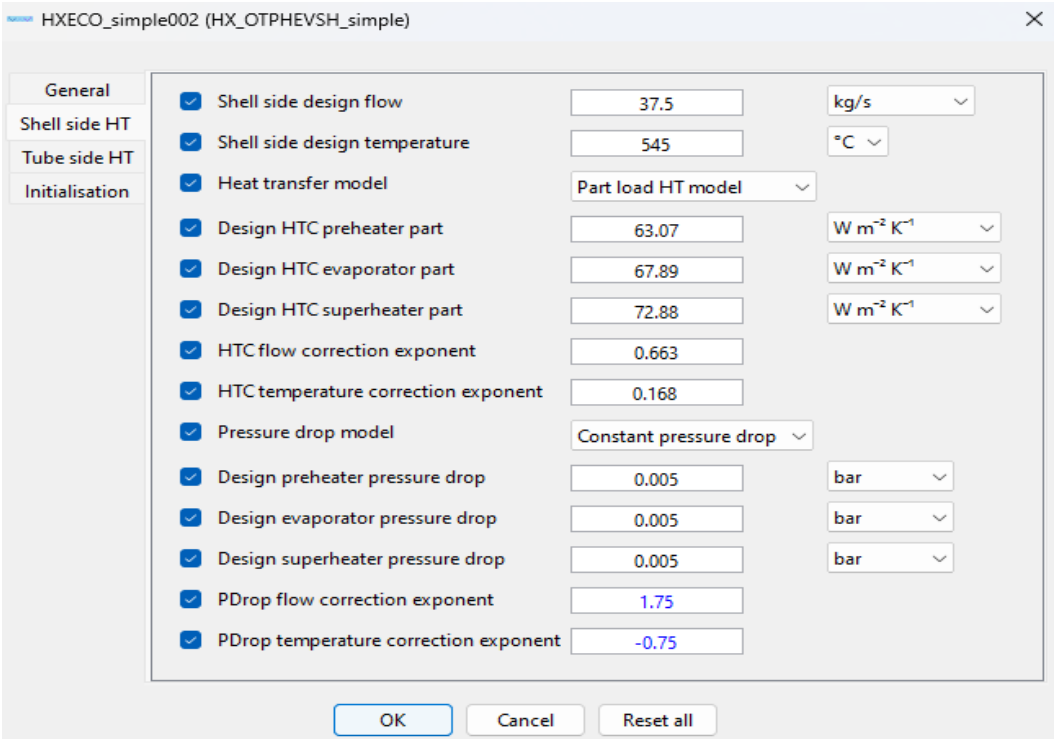

Figure 9. Insert of coefficient values in the outside part of the heat exchanger

Last but not least, the operating pressure of the steam cycle has to be set as follows:

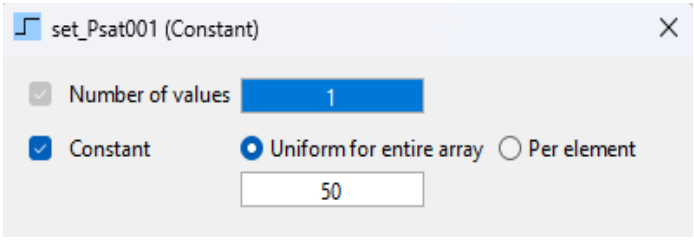

Figure 10. Insert of operating pressure of the steam cycle

4.3 Steam Turbine

In order to model the operation of the steam turbine is necessary to set its isentropic efficiency. Because of lack of information about the isentropic efficiency, it is necessary to test various values to find the appropriate value. The comparative basis for this selection is the operating data from the manufacturer in order to compare the produced power in the program and in the data sheet of the manufacturer.

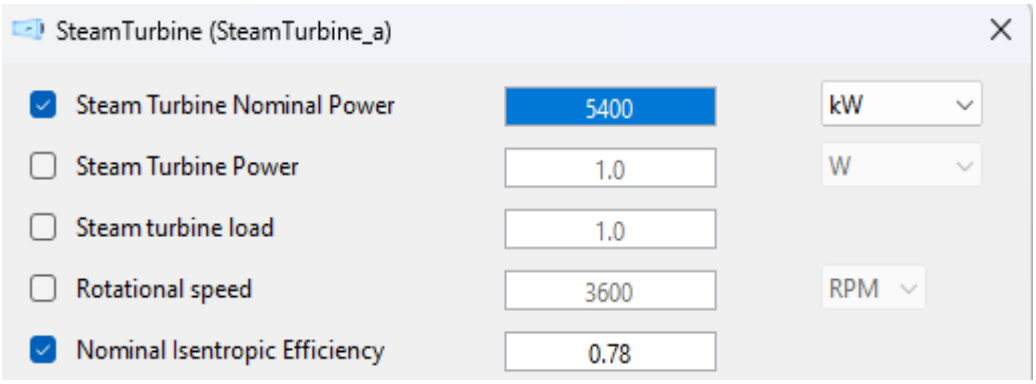

Figure 11. Insert of isentropic efficiency in the steam turbine

4.4 Complete System Model

Connecting the referred components of the installation and adding various sub-components, it is created the whole system model as it is depicted below:

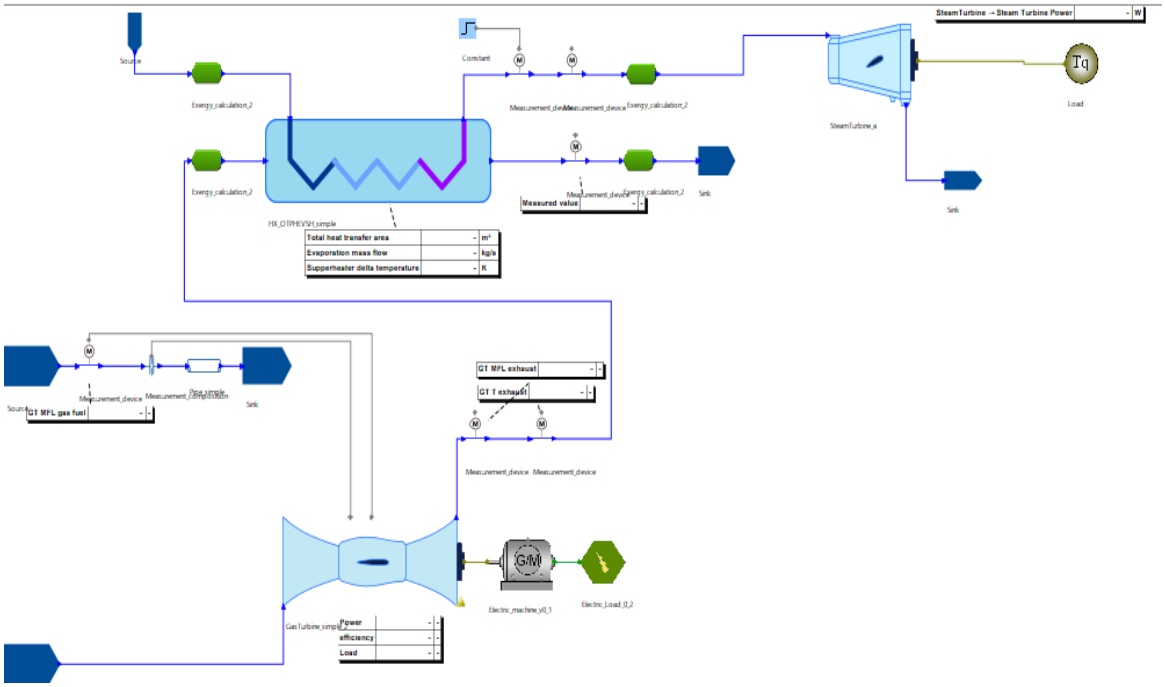

Figure 12. Complete System Model in GProms

4.5 Optimization of the COGES System

After the setup of the complete system. an optimization methos was carried out in the, GProms in order to be defined the value of the parameters, which maximize the produced power of the COGES. These parameters were the high operating pressure of the steam cycle and the temperature difference between the exhaust gas and the steam in the once-through heat exchanger in ISO and Tropical conditions. The considered range for the high pressure was 40-50 bar and as it was examined the total power increases as the pressure increases, so the selected pressure value was 50 bar for each load of the gas turbine. Concerning the superheating degree, the considered range was 15-50 ºC. The optimization process was carried out for methanol, LNG and hydrogen as fuels of the gas turbine and the results are illustrated below.

Table 15. Optimized Parameters of the COGES using Methanol as fuel

		OPTIMIZED PARAMETERS-METHANOL	
ΣΥΝΘΗΚΕΣ	**ΦΟΡΤΙΟ**	**$Pressure_{STEAM}$**	**T_{GAS}-T_{ST}**
ISO CONDITIONS	**100%**	50	15
	90%	50	15
	80%	50	15
	70%	50	15
	60%	50	13.4
	50%	50	18.7
TROPICAL CONDITIONS	**100%**	50	25.3
	90%	50	16.1
	80%	50	22.5
	70%	50	28.7
	60%	50	34.2
	50%	50	40.2

Table 16. Optimized Parameters of the COGES using LNG as fuel

		OPTIMIZED PARAMETERS-LNG	
ΣΥΝΘΗΚΕΣ	**ΦΟΡΤΙΟ**	**$Pressure_{STEAM}$**	**T_{GAS}-T_{ST}**
ISO CONDITIONS	**100%**	50	31
	90%	50	23.5
	80%	50	29.8
	70%	50	35
	60%	50	40.2
	50%	50	45.4
TROPICAL CONDITIONS	**100%**	50	15
	90%	50	15
	80%	50	15
	70%	50	15
	60%	50	15
	50%	50	18.9

Table 17. Optimized Parameters of the COGES using Hydrogen as fuel

		OPTIMIZED PARAMETERS-HYDROGEN	
ΣΥΝΘΗΚΕΣ	**ΦΟΡΤΙΟ**	**$Pressure_{STEAM}$**	**T_{GAS}-T_{ST}**
ISO CONDITIONS	**100%**	50	19.6
	90%	50	12.1
	80%	50	18.4
	70%	50	23.5
	60%	50	29
	50%	50	29.58
TROPICAL CONDITIONS	**100%**	50	15
	90%	50	15
	80%	50	15
	70%	50	15
	60%	50	15
	50%	50	15

5. Case Study Analysis

In order to investigate the feasibility of using the COGES, a case study will be carried out where the combined system will be used on a cruise ship of the Carnival company of the Aida series of ships. Before we proceed to the case study, some data will be listed regarding the under-examination ship Aida Perla. Then the particular ship's profile of sailing hours and power demand over a period of one year will be listed. Afterwards based on the power requirements. a plan will be drawn up to use the combined system with the ship's existing gas turbines in order to optimize the plant's performance and maximize fuel savings.

5.1 Ship Case Study

The AIDA Perla is a cruise ship owned by Carnival Corporation & plc and operated by AIDA Cruises, a German cruise line catering primarily to the German-speaking market. The AIDA Perla measures approximately 300 meters in length, with a beam of 37.6 meters. The ship has a gross tonnage of around 125.572 GT (gross tonnage). It has a capacity of around 3.286 passengers and about 900 crew members. AIDA Perla was built by Mitsubishi Heavy Industries at their shipyard in Nagasaki, Japan. and delivered in 2017. It is the second ship in AIDA's Hyperion-class, following its sister ship, AIDA Prima. The design reflects a modern, sleek profile with an emphasis on energy efficiency and environmental sustainability. AIDA Perla operates various itineraries, primarily focusing on the Mediterranean. Canary Islands and Northern Europe. Cruises typically range from 7 to 14 days, visiting major cities, scenic coastal towns and culturally significant ports. Popular itineraries include stops in Spain, Italy, Portugal, France and the Canary Islands. AIDA Perla reflects AIDA Cruises' commitment to sustainability. Its use of LNG in ports, advanced air lubrication technology, energy-efficient systems, and comprehensive waste management facilities underscore its focus on reducing environmental impact. However, the ship like all cruise vessels, is still subject to scrutiny concerning its overall ecological footprint, especially in sensitive environments and due to this reason a COGES system is proposed in order to be able to utilize alternative fuels and reduce its ecological footprint.

Figure 13. Aida Perla Cruise Ship

5.2 Statistical Features

Next, the statistics of the required propulsion power of the ship under consideration are listed over the period of one year. As can be noticed. most of the hours are done at a power of 9000 and 16000-19000 kW.

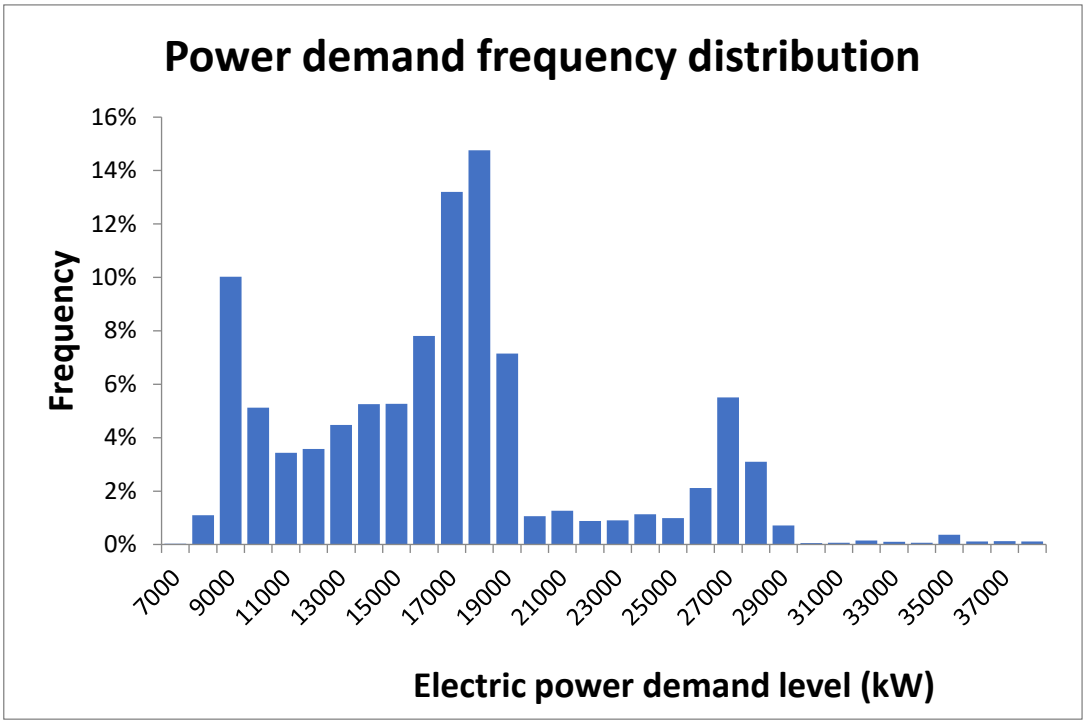

Figure 14. Electric Power demand of Aida Perla on annual basis

5.3 Examined Propulsion Plants Features

The propulsion systems considered are the COGES, which is discussed at length in chapter 4, as well as the 6L46TS-DF and 9L46TS-DF engines. The mentioned diesel engines are analyzed in the following subsections.

5.3.1 6L46TS-DF

The 6L46TS-DF engine is part of a series of marine engines designed for high efficiency and reduced emissions, typically used in applications such as cruise ships. Ferries, and other large vessels. The 6L46TS-DF is produced by Wartsila, is a medium-speed dual-fuel engine that can operate on both heavy fuel oil (HFO) or marine diesel oil (MDO) and liquefied natural gas (LNG). It is a 6-cylinder in-line engine and has a rated power output typically ranging from 5,400 to 5,800 kW (approximately 7,240 to 7,780 hp), depending on its configuration and specific operating conditions. It is designed as a medium-speed engine, usually operating in the range of 500 to 600 RPM**.** The engine is optimized for high thermal efficiency, which reduces fuel consumption and operational costs over long voyages.

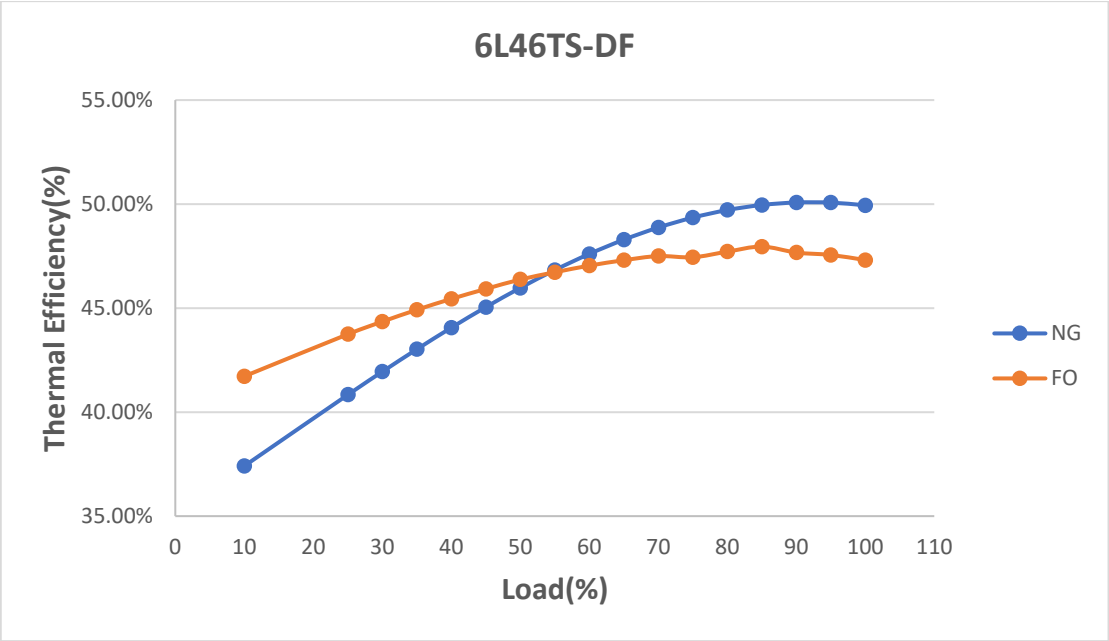

Figure 15. Diagram of thermal efficiency-load for 6L46TS-DF with NG and FO

5.3.2 9L46TS-DF

The 9L46TS-DF is manufactured by Wärtsilä and is a medium-speed, four-stroke, dual-fuel engine. It is designed to operate on both conventional marine fuels (like Marine Diesel Oil (MDO) or Heavy Fuel Oil (HFO)) and LNG, offering fuel flexibility depending on availability and environmental regulations. The 9L46TS-DF engine typically delivers a power output of 9,000 kW to 9,900 kW (approximately 12.000 to 13.200 hp). The engine operates at medium speeds, generally in the range of 500 to 600 RPM**.** The engine meets IMO Tier III emission standards when operating on LNG, allowing it to operate in Emission Control Areas (ECAs) without requiring additional exhaust gas after-treatment systems. Utilizes both a high-pressure common rail system for liquid fuel and a gas admission valve system for LNG.

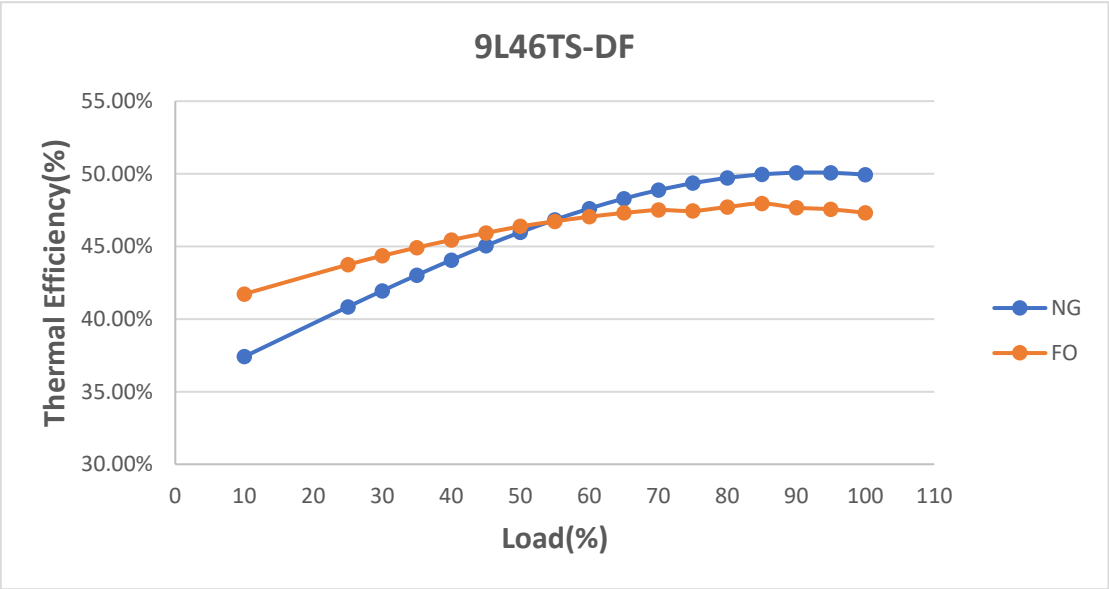

Figure 16. Diagram of thermal efficiency-load for 9L46TS-DF with NG and FO

5.4 COGES Performance per Load and Fuel

The designed COGES system was tested for several Loads and Fuels in the gProms platform. Target of this analysis was to depict the performance of the combined system on a wide range of loads using alternative fuels. The key examined operating parameters were the following:

- the produced power of the Gas Turbine (GT Power)
- the produced power of the Steam Turbine (ST Power)
- the total produced power of the COGES (COGES Power)
- the thermal efficiency of the Gas Turbine (n_{GT})
- the total thermal efficiency (n_{TOTAL})
- the specific fuel consumption of the Gas Turbine ($bsfc_{initial}$)
- the total specific fuel consumption ($bsfc_{final}$)
- the temperature of the exhaust gas after the Gas Turbine (**$T_{gasafter\ GT}$**)
- the temperature of the exhaust gas after the once-through boiler (**$T_{gasfinal}$**)
- the temperature of the steam after the once-through boiler (**T_{st}**)
- the mass flow rate of the exhaust gas (m_{gas})
- the mass flow rate of the steam (m_{st})
- the operating pressure of the steam cycle (P_{ST})
- the temperature difference between the exahust gas and the steam (T_{GAS}-T_{ST})

5.4.1 COGES with Hydrogen

Firstly, the operation of COGES was studied at loads of 50-100% of the MCR of the gas turbine using hydrogen as fuel and the results are depicted in the following Table. The produces power in the steam turbine ranges from 4,087 to 4,952 kW. The overall efficiency ranges from 43.2-49.22% with the improvement over the gas turbine efficiency ranging from 46.08-76.06%. The improvement in specific fuel consumption ranges from 32.2-43.95%. Moreover, operational characteristics of COGES are listed in the following table as well as the fuel and steam supplies in the considered load range.

Table 18. COGES Performance with Hydrogen on various loads

Load(%)	Heat Input(kW)	GT Power(kW)	ST Power(kW)	COGES Power(kW)	GT Power(kW)/ ST Power(kW)
100	30939.56	10425.66	4952.37	15378.03	2.11
90	28643.35	9383.09	4620.46	14003.55	2.03
80	26584.98	8340.53	4525.65	12866.17	1.84
70	24704.57	7297.96	4397.72	11695.68	1.66
60	22945.50	6255.39	4261.40	10516.80	1.47
50	21245.48	5212.83	4087.53	9300.35	1.28

Load(%)	n_{total}(%)	n_{GT}(%)	$n_{improvement}$(%)	m_{fuel}(kg/s)	$bsfc_{initial}$(gr/kWh)
100	49.22%	33.70%	46.08%	0.26	89.06
90	48.41%	32.76%	47.77%	0.24	91.61
80	47.89%	31.37%	52.63%	0.22	95.66
70	46.81%	29.54%	58.45%	0.21	101.59
60	45.28%	27.26%	66.08%	0.19	110.08
50	43.20%	24.54%	76.06%	0.18	122.31

Load(%)	$T_{gasafter\ GT}$(C)	$bsfc_{final}$(gr/kWh)	bsfc $_{improvement}$(%)	m_{steam}(kg/sec)	T_{st}(C)
100	544.56	60.38	32.20%	4.64	525.00
90	537.13	61.38	32.99%	4.35	520.58
80	543.36	62.01	35.17%	4.24	525.00
70	548.48	63.39	37.60%	4.12	525.00
60	554.00	65.48	40.52%	3.99	525.00
50	558.01	68.55	43.95%	3.83	525.00

Load(%)	m_{gas}(kg/s)	$T_{gasfinal}$(C)	DT_{SUP}(C)	Pst(bar)	
100	34.38	145.86	19.56	50.00	
90	33.04	148.38	16.55	50.00	
80	31.65	145.95	18.36	50.00	
70	30.21	143.41	23.48	50.00	
60	28.71	140.69	29.00	50.00	
50	27.17	138.65	33.01	50.00	

5.4.2 COGES with Methanol

Subsequently, the operation of COGES was studied at loads of 50-100% of the MCR of the gas turbine using Methanol as fuel and the results are illustrated in the following Table. The produces power in the steam turbine ranges from 4,089 to 4,945 kW. The overall efficiency ranges from 42.46-48.07% with the improvement over the gas turbine efficiency ranging from 48.32-79.91%.

The improvement in specific fuel consumption ranges from 33.25-45.17%. Furthermore, operational characteristics of COGES are listed in the following table as well as the fuel and steam supplies in the considered load range.

Table 19. COGES Performance with Methanol on various loads

Load(%)	Heat Input(kW)	GT Power(kW)	ST Power(kW)	COGES Power(kW)	GT Power(kW)/ ST Power(kW)
100	30629.06	9927.16	4945.54	14872.70	2.01
90	28355.90	8934.45	4615.35	13549.80	1.94
80	26318.18	7941.73	4522.82	12464.55	1.76
70	24456.64	6949.02	4396.75	11345.77	1.58
60	22715.23	5956.30	4261.98	10218.28	1.40
50	21032.27	4963.58	4089.29	9052.87	1.21

Load(%)	n_{total}(%)	n_{GT}(%)	$n_{improvement}$(%)	m_{fuel}(kg/s)	$bsfc_{initial}$(gr/kWh)
100	48.07%	32.41%	48.32%	1.54	557.32
90	47.30%	31.51%	50.11%	1.42	573.29
80	46.85%	30.18%	55.24%	1.32	598.60
70	45.85%	28.41%	61.37%	1.23	635.72
60	44.42%	26.22%	69.41%	1.14	688.87
50	42.46%	23.60%	79.91%	1.06	765.40

Load(%)	$T_{gasafter\ GT}$(C)	$bsfc_{final}$(gr/kWh)	bsfc $_{improvement}$(%)	m_{steam}(kg/sec)	T_{st}(C)
100	542.83	372.00	33.25%	4.63	525.00
90	535.42	378.01	34.06%	4.35	519.16
80	541.63	381.39	36.29%	4.24	525.00
70	546.74	389.37	38.75%	4.12	525.00
60	552.25	401.55	41.71%	3.99	525.00
50	556.26	419.66	45.17%	3.83	525.00

Load(%)	m_{gas}(kg/s)	$T_{gasfinal}$(C)	DT_{SUP}(C)	P_{st}(bar)	
100	35.00	146.19	17.83	50.00	
90	33.64	148.56	16.27	50.00	
80	32.23	146.33	16.63	50.00	
70	30.76	143.79	21.74	50.00	
60	29.24	141.07	27.25	50.00	
50	27.66	139.04	31.26	50.00	

5.4.3 COGES with Natural Gas

Furthermore, the operation of COGES was studied at loads of 50-100% of the MCR of the gas turbine using Natural Gas as fuel and the results are illustrated in the following Table. The produced power in the steam turbine ranges from 4,039 to 4,892 kW. The overall efficiency ranges from 43.13-48.61% with the improvement over the gas turbine efficiency ranging from 50.44-83.31%. The improvement in specific fuel consumption ranges from 34.21-46.20%. In addition, operational characteristics of COGES are illustrated in the following table as well as the fuel and steam mass flow rates in the considered load range.

Table 20. COGES Performance with Natural Gas on various loads

Load (%)	Heat Input(kW)	GT Power(kW)	ST Power(kW)	COGES Power(kW)	GT Power(kW)/ ST Power(kW)
100	29114.10	9407.79	4892.03	14299.81	1.92
90	26953.37	8467.01	4570.98	13037.99	1.85
80	25016.44	7526.23	4475.61	12001.84	1.68
70	23246.97	6585.45	4348.10	10933.55	1.51
60	21591.69	5644.67	4212.17	9856.84	1.34
50	19991.98	4703.89	4039.86	8743.75	1.16

Load (%)	n_{total}(%)	n_{GT}(%)	$n_{improvement}$(%)	m_{fuel}(kg/s)	$bsfc_{initial}$(gr/kWh)
100	48.61%	32.31%	50.44%	0.52	198.32
90	47.86%	31.41%	52.37%	0.48	204.00
80	47.44%	30.09%	57.68%	0.45	213.01
70	46.47%	28.33%	64.05%	0.41	226.22
60	45.07%	26.14%	72.38%	0.38	245.13
50	43.13%	23.53%	83.31%	0.36	272.37

Load (%)	$T_{gasafter\ GT}$(C)	$bsfc_{final}$(gr/kWh)	bsfc $_{improvement}$(%)	m_{steam}(kg/sec)	T_{st}(C)
100	556.04	130.47	34.21%	4.58	525.00
90	548.51	132.48	35.06%	4.28	525.00
80	554.82	133.58	37.29%	4.19	525.00
70	560.01	136.26	39.77%	4.07	525.00
60	565.60	140.38	42.73%	3.95	525.00
50	569.68	146.53	46.20%	3.78	525.00

Load (%)	m_{gas}(kg/s)	$T_{gasfinal}$(C)	DTSUP(C)	Pst(bar)	
100	33.12	140.12	31.04	50.00	
90	31.83	143.27	23.51	50.00	
80	30.49	140.24	29.82	50.00	
70	29.10	137.72	35.01	50.00	
60	27.66	135.01	40.60	50.00	
50	26.17	132.96	44.68	50.00	

5.4.4 COGES with Mixture of 80% Hydrogen and 20% Natural Gas

In addition, the operation of COGES was studied at loads of 50-100% of the MCR of the gas turbine using a Mixture of 80% Hydrogen and 20% Natural Gas as fuel and the results are depicted in the following Table. The produced power in the steam turbine ranges from 4,082 to 4,948 kW. The overall efficiency ranges from 43.27-49.04% with the improvement over the gas turbine efficiency ranging from 48.28-79.66%. The improvement in specific fuel consumption ranges from 33.23-45.09%. Furthermore, operational characteristics of COGES are illustrated in the following table as well as the fuel and steam mass flow rates in the considered load range.

Table 21. COGES Performance with Mixture of 80% Hydrogen and 20% Natural Gas on various loads

Load (%)	Heat Input(kW)	GT Power(kW)	ST Power(kW)	COGES Power(kW)	GT Power(kW)/ ST Power(kW)
100	30059.51	9941.69	4948.00	14889.69	2.01
90	27828.61	8947.52	4618.79	13566.31	1.94
80	25828.79	7953.35	4522.60	12475.95	1.76
70	24001.86	6959.18	4393.71	11352.90	1.58
60	22292.83	5965.02	4256.52	10221.54	1.40
50	20641.17	4970.85	4082.25	9053.10	1.22

Load (%)	n_{total}(%)	n_{GT}(%)	$n_{improvement}$(%)	m_{fuel}(kg/s)	$bsfc_{initial}$(gr/kWh)
100	49.04%	33.07%	48.28%	0.28	102.79
90	48.25%	32.15%	50.07%	0.26	105.73
80	47.78%	30.79%	55.16%	0.24	110.40
70	46.75%	28.99%	61.24%	0.23	117.25
60	45.28%	26.76%	69.22%	0.21	127.05
50	43.27%	24.08%	79.66%	0.19	141.16

Load (%)	$T_{gasafter\ GT}$(C)	$bsfc_{final}$(gr/kWh)	bsfc $_{improvement}$(%)	m_{steam}(kg/sec)	T_{st}(C)
100	549.74	68.63	33.23%	4.64	525.00
90	542.27	69.73	34.05%	4.33	525.00
80	548.53	70.38	36.25%	4.24	525.00
70	553.68	71.87	38.70%	4.12	525.00
60	559.24	74.14	41.64%	3.99	525.00
50	563.28	77.51	45.09%	3.82	525.00
Load (%)	**m_{gas}(kg/s)**	**$T_{gasfinal}$(C)**	**DTSUP(C)**	**Pst(bar)**	
100	33.78	143.39	24.74	50.00	
90	32.46	146.53	17.27	50.00	
80	31.10	143.48	23.53	50.00	
70	29.68	140.95	28.68	50.00	
60	28.22	138.24	34.24	50.00	
50	26.70	136.19	38.28	50.00	

5.4.5 COGES with Mixture of 70% Hydrogen and 30% Natural Gas

Moreover, the operation of COGES was studied at loads of 50-100% of the MCR of the gas turbine using a Mixture of 70% Hydrogen and 30% Natural Gas as fuel and the results are shown in the following Table. The produced power in the steam turbine ranges from 4,080 to 4,946 kW. The overall efficiency ranges from 43.27-48.97% with the improvement over the gas turbine efficiency ranging from 48.94-80.75%. The improvement in specific fuel consumption ranges from 33.54-45.43%. Furthermore, operational characteristics of COGES are illustrated in the following table as well as the fuel and steam mass flow rates in the considered load range.

Table 22. COGES Performance with Mixture of 70% Hydrogen and 30% Natural Gas on various loads

Load (%)	Heat Input(kW)	GT Power(kW)	ST Power(kW)	COGES Power(kW)	GT Power(kW)/ ST Power(kW)
100	29815.10	9802.77	4946.13	14748.89	1.98
90	27602.34	8822.49	4617.88	13440.37	1.91
80	25618.78	7842.21	4521.33	12363.54	1.73
70	23806.71	6861.94	4392.23	11254.17	1.56
60	22111.57	5881.66	4254.84	10136.51	1.38
50	20473.34	4901.38	4080.50	8981.89	1.20

Load (%)	n_{total}(%)	n_{GT}(%)	$n_{improvement}$(%)	m_{fuel}(kg/s)	$bsfc_{initial}$(gr/kWh)
100	48.97%	32.88%	48.94%	0.30	110.75
90	48.19%	31.96%	50.77%	0.28	113.92
80	47.73%	30.61%	55.92%	0.26	118.95
70	46.72%	28.82%	62.09%	0.24	126.33
60	45.27%	26.60%	70.17%	0.22	136.89
50	43.27%	23.94%	80.75%	0.21	152.09

Load (%)	$T_{gasafter\ GT}$(C)	$bsfc_{final}$(gr/kWh)	$bsfc_{improvement}$(%)	m_{steam}(kg/sec)	T_{st}(C)
100	551.36	73.61	33.54%	4.63	525.00
90	543.88	74.78	34.36%	4.33	525.00

80	550.15	75.45	36.57%	4.24	525.00
70	555.31	77.02	39.03%	4.11	525.00
60	560.88	79.43	41.98%	3.99	525.00
50	564.93	83.00	45.43%	3.82	525.00
Load (%)	**m_{gas}(kg/s)**	**$T_{gasfinal}$(C)**	**DT_{SUP}(C)**	**P_{st}(bar)**	
100	33.61	142.61	26.36	50.00	
90	32.30	145.75	18.88	50.00	
80	30.94	142.70	25.15	50.00	
70	29.53	140.17	30.31	50.00	
60	28.07	137.46	35.88	50.00	
50	26.56	135.41	39.93	50.00	

5.4.6 Summary of the Results

As can be easily seen, the addition of the Steam Turbine and the Once-through Boiler for the exploitation of the gas turbine exhaust gases leads to significant increase in the thermal efficiency of the system, which ranges in all cases examined from 46% to 83 %. At high loads the power output of the steam turbine is about half that of the gas turbine but as the loads decrease the power output of the steam turbine ends up being about 80% of the power of the gas turbine. Also, the specific fuel consumption shows a significant improvement in the combined system compared to the simple system, ranging from 32%-46%. In addition, the power produced in the steam turbine is observed to be maximized in the cases of fuel mixtures, in which it reaches almost 4950 kW. As can be seen in Figure 17, the total efficiency of the COGES ranges from 42% to 49% for different fuels and loads. As the load increases, the total efficiency increases and it should be referred that the lowest values are depicted for the COGES with Methanol and the highest values for the COGES with the fuel mixture of 70% Hydrogen and 30% Natural Gas.

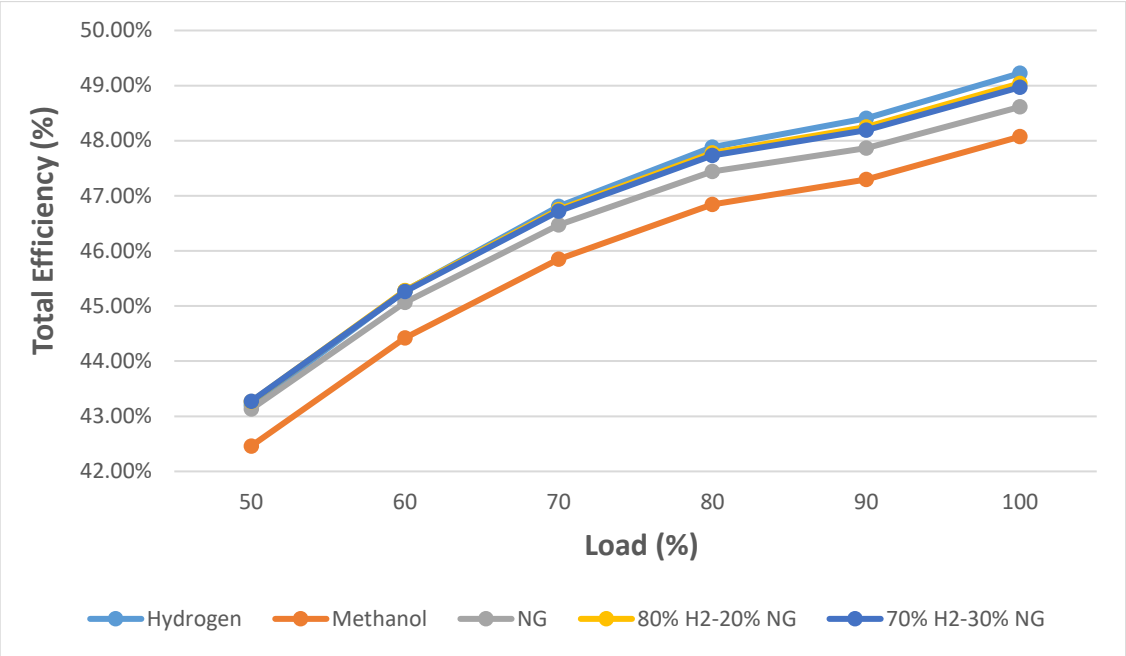

Figure 17. Total Efficiency-Load Diagram of the COGES for different Fuels

5.5 Methodology Description

The purpose of the case study was to present the potential of COGES in covering the energy needs of the ship under study, the capability to use many alternative fuels in the gas turbine and the recording of the performance of the examined propulsion systems in comparison to conventional propulsion systems. More specifically, 5 different fuels for the gas turbine were examined, which were also analyzed in chapter 5.4. Moreover, along with the 2 gas turbines that were part of COGES, another 4 diesel engines were used, 2 6L46TS-DF and 2 9L46TS-DF, which were able to use natural gas and methanol as fuel and used having a dual role. They were initially used as a full conventional propulsion scheme in order to be compared with the systems containing the COGES and subsequently used as a supplement to the COGES systems when their power was insufficient to cover the electrical needs. To be able to operate the COGES with a comparable degree of efficiency in relation to a modern diesel engine, it should operate at loads of 70% and above, where its efficiency exceeds 46% as it was illustrated in chapter 5.4. For this reason, a strategy was adopted in which when the power requirement did not reach 70% of one COGES or when it was above 70% for only one of the two COGES, one 9L46TS-DF diesel engine operated. In addition, under the same strategy when the conditions for the use of both COGES were fulfilled, then there was an equal sharing of the distributed loads and the load percentage of the gas turbines did not exceed 95% of the MCR in any case.

The propulsion scenarios considered for the various fuels are as follows:

• Case 01: 2x6L46TS-DF and 2x9L46TS-DF fuel MGO

• Case 02: 2x6L46TS-DF and 2x9L46TS-DF with Natural Gas

• Case 03: 2x6L46TS-DF and 2x9L46TS-DF with Methanol

• Case 04: 2xCOGES with Hydrogen and 1x9L46TS-DF with Natural Gas

• Case 05: 2xCOGES with Hydrogen and 1x9L46TS-DF with Methanol

• Case 06: 2xCOGES with Hydrogen and 1x9L46TS-DF with MGO

• Case 07: 2xCOGES with Methanol and 1x9L46TS-DF with Natural Gas

• Case 08: 2xCOGES with Methanol and 1x9L46TS-DF with Methanol

• Case 09: 2xCOGES with Methanol and 1x9L46TS-DF with MGO

• Case 10: 2xCOGES with Natural Gas and 1x9L46TS-DF with Natural Gas

• Case 11: 2xCOGES with Natural Gas and 1x9L46TS-DF with Methanol

• Case 12: 2xCOGES with Natural Gas and 1x9L46TS-DF with MGO

• Case 13: 2xCOGES with a mixture of 70% Hydrogen - 30% Natural Gas and 1x9L46TS-DF with Natural Gas

• Case 14: 2xCOGES with a mixture of 70% Hydrogen - 30% Natural Gas and 1x9L46TS-DF with Methanol

• Case 15: 2xCOGES with a mixture of 70% Hydrogen - 30% Natural Gas and 1x9L46TS-DF with MGO

• Case 16: 2xCOGES with a mixture of 80% Hydrogen - 20% Natural Gas and 1 9L46TS-DF with Natural Gas

• Case 17: 2xCOGES with a mixture of 80% Hydrogen - 20% Natural Gas and 1x9L46TS-DF with Methanol

• Case 18: 2xCOGES with a mixture of 80% Hydrogen - 20% Natural Gas and 1x9L46TS-DF with MGO

5.6 COGES HRSG Off-Design Performance Analysis

As it was referred in the previous chapter, the power demands of the studied vessel were covered with a combination of COGES systems and Diesel Engines. The utilized data was the Performance Analysis of the COGES system and the performance data of the diesel engines manufacturer. It was necessary to use off-design points of operation for the examined engines in order to cover the necessary power demands and for that reason polynomial correlations were created in order to describe these points. These equations were third degree polynomials and their accuracy was almost 99.9%, therefore they could give highly reliable values at off-design operating points. An example of these equations is given in the following diagram with the fuel consumption(hydrogen) of the gas turbine.

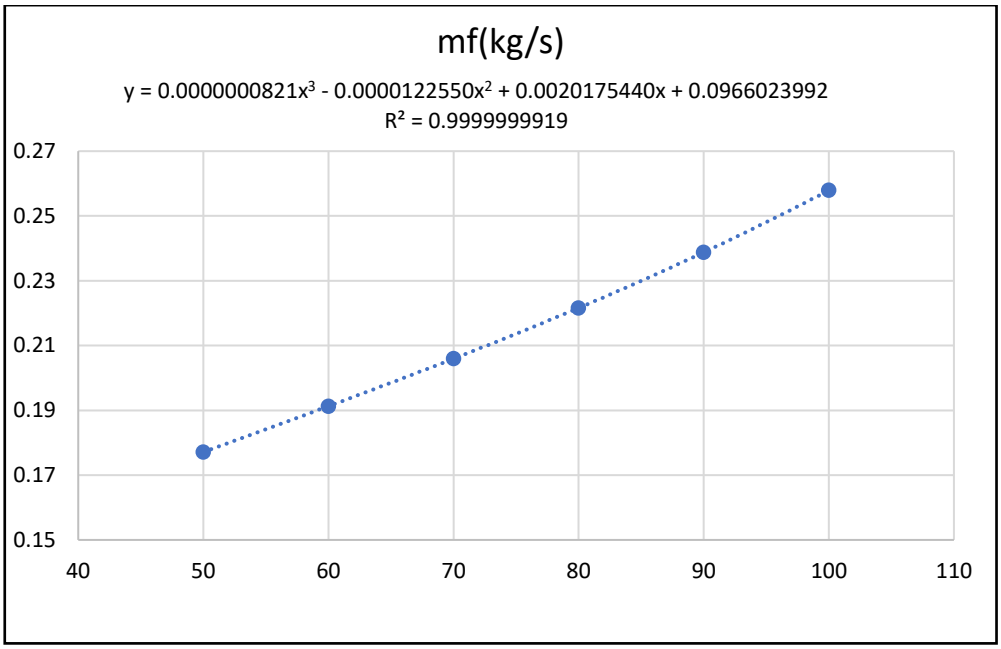

Figure 18. Off-Design Correlation for the fuel consumption of the Gas Turbine

6. Case Study Results

The results obtained from the case study for the various cases are listed below where the consumptions of each fuel used on an annual basis, the total carbon dioxide emissions for each case on an annual basis as well as the total fuel cost for each scenario are analyzed. The obtained fuel prices are listed in table 23 while the CO2 emission factors are presented in table 24.

Table 23. Price for each examined fuel

Fuel Prices	
Price of Hydrogen ($/Ton)	**2500**
Price of Natural Gas ($/Ton)	**1100**
Price of Methanol ($/Ton)	**450**
Price of MGO ($/Ton)	**640**

Table 24. CO_2 emission factor for each examined fuel

CO_2 Emission Factors (Tons CO_2/Tons Fuel)	
DIESEL	3.206
NATURAL GAS	2.784
HYDROGEN	0.09
METHANOL	1.384
70 NG-30 H2	2.220
80 H_2-20 NG	1.942

6.1 2x6L46TS-DF and 2x9L46TS-DF with MGO

Initially, the results of the first studied case of the case study will be listed, which uses 2 6L46TS-DF and 2 9L46TS-DF with MGO for fuel as a propulsion plant during one year and are illustrated in Table 25.

Table 25. Annual fuel consumption, total CO_2 emissions, total annual fuel cost for case 2 6L46TS-DF and 2 9L46TS-DF with MGO

2 6L46TS-DF AND 2 9L46TS-DF WITH MGO					
AVERAGE $N_{OVERALL}$	ANNUAL CONS. OF HYDROGEN (TONS)	ANNUAL CONS. OF NATURAL GAS (TONS)	ANNUAL CONS. OF METHANOL (TONS)	ANNUAL CONS. OF MGO (TONS)	TOTAL CO_2 EMISSIONS (TONS)
48.14%	0.00	0.00	0.00	14990.93	48060.9
	ANNUAL COST OF HYDROGEN ($)	ANNUAL COST OF NATURAL GAS ($)	ANNUAL COST OF METHANOL ($)	ANNUAL COST OF MGO ($)	TOTAL ANNUAL FUEL COST ($)
	0.00	0.00	0.00	9,594,193.62	9,594,193.62

6.2 2 6L46TS-DF and 2 9L46TS-DF with Natural Gas

The results of the case study scenario, which uses 2 6L46TS-DF and 2 9L46TS-DF, with Natural Gas for fuel, as a propulsion plant during one year are illustrated in Table 26.

Table 26. Annual fuel consumption, total CO_2 emissions, total annual fuel cost for case 2 6L46TS-DF and 2 9L46TS-DF with Natural Gas

2 6L46TS-DF AND 2 9L46TS-DF WITH NATURAL GAS					
AVERAGE $N_{OVERALL}$	ANNUAL CONS. OF HYDROGEN (TONS)	ANNUAL CONS.OF NATURAL GAS (TONS)	ANNUAL CONS. OF METHANOL (TONS)	ANNUAL CONS. OF MGO (TONS)	TOTAL CO_2 EMISSIONS (TONS)
49.42%	0.00	12425.06	0.00	116.21	34963.96
	ANNUAL COST OF HYDROGEN($)	ANNUAL COST OF NATURAL GAS ($)	ANNUAL COST OF METHANOL($)	ANNUAL COST OF MGO ($)	TOTAL ANNUAL FUEL COST ($)
	0.00	13,667,570.36	0.00	74,376.81	13,741,947.16

6.3 2 6L46TS-DF and 2 9L46TS-DF with Methanol

The results of the case study scenario, which uses 2 6L46TS-DF and 2 9L46TS-DF, with Methanol for fuel, as a propulsion plant during one year are illustrated in Table 27.

Table 27. Annual fuel consumption, total CO_2 emissions, total annual fuel cost for case 2 6L46TS-DF and 2 9L46TS-DF with Methanol

2 6L46TS-DF AND 2 9L46TS-DF WITH METHANOL					
AVERAGE $N_{OVERALL}$	ANNUAL CONS. OF HYDROGEN (TONS)	ANNUAL CONS. OF NATURAL GAS (TONS)	ANNUAL CONS. OF METHANOL (TONS)	ANNUAL CONS. OF MGO (TONS)	TOTAL CO_2 EMISSIONS (TONS)
49.42%	0.00	0.00	30975.26	116.21	43249.92
	ANNUAL COST OF HYDROGEN ($)	ANNUAL COST OF NATURAL GAS ($)	ANNUAL COST OF METHANOL ($)	ANNUAL COST OF MGO ($)	TOTAL ANNUAL FUEL COST ($)
	0.00	0.00	13,938,869.23	74,376.81	14,013,246.04

6.4 2 COGES with Hydrogen and 1 9L46TS-DF with Natural Gas

The results of the case study scenario, which uses 2 COGES, with Hydrogen for fuel and 1L46TS-DF, with Natural Gas for fuel, as a propulsion plant during one year are illustrated in Table 28.

Table 28. Annual fuel consumption, total CO_2 emissions, total annual fuel cost for case 2 COGES with Hydrogen and 1 9L46TS-DF with Natural Gas

2 COGES WITH HYDROGEN AND 1 9L46TS-DF WITH NATURAL GAS					
AVERAGE $N_{OVERALL}$	ANNUAL CONS. OF HYDROGEN (TONS)	ANNUAL CONS. OF NATURAL GAS (TONS)	ANNUAL CONS. OF METHANOL (TONS)	ANNUAL CONS. OF MGO (TONS)	TOTAL CO_2 EMISSIONS (TONS)
47.69%	4144.95	3037.93	0.00	74.50	9069.48
	ANNUAL COST OF HYDROGEN ($)	ANNUAL COST OF NATURAL GAS ($)	ANNUAL COST OF METHANOL ($)	ANNUAL COST OF MGO ($)	TOTAL ANNUAL FUEL COST ($)
	10,362,364.19	3,341,719.34	0.00	47,680.72	13,751,764.25

6.5 2 COGES with Hydrogen and 1 9L46TS-DF with Methanol

The results of the case study scenario, which uses 2 COGES, with Hydrogen for fuel and 1L46TS-DF, with Methanol for fuel, as a propulsion plant during one year are illustrated in Table 29.

Table 29. Annual fuel consumption, total CO_2 emissions, total annual fuel cost for case 2 COGES with Hydrogen and 1 9L46TS-DF with Methanol

2 COGES WITH HYDROGEN AND 1 9L46TS-DF WITH METHANOL					
AVERAGE $N_{OVERALL}$	ANNUAL CONS. OF HYDROGEN (TONS)	ANNUAL CONS. OF NATURAL GAS (TONS)	ANNUAL CONS. OF METHANOL (TONS)	ANNUAL CONS. OF MGO (TONS)	TOTAL CO_2 EMISSIONS (TONS)
47.69%	4144.95	0.00	7573.45	74.50	11095.40
	ANNUAL COST OF HYDROGEN ($)	ANNUAL COST OF NATURAL GAS ($)	ANNUAL COST OF METHANOL ($)	ANNUAL COST OF MGO ($)	TOTAL ANNUAL FUEL COST ($)
	10,362,364.19	0.00	3,408,051.88	47,680.72	13,818,096.79

6.6 2 COGES with Hydrogen and 1 9L46TS-DF with MGO

The results of the case study scenario, which uses 2 COGES, with Hydrogen for fuel and 1L46TS-DF, with MGO for fuel, as a propulsion plant for one year are illustrated in Table 30.

Table 30. Annual fuel consumption, total CO_2 emissions, total annual fuel cost for case 2 COGES with Hydrogen and 1 9L46TS-DF with MGO

2 COGES WITH HYDROGEN AND 1 9L46TS-DF WITH MGO					
AVERAGE $N_{OVERALL}$	ANNUAL CONS. OF HYDROGEN (TONS)	ANNUAL CONS. OF NATURAL GAS (TONS)	ANNUAL CONS. OF METHANOL (TONS)	ANNUAL CONS. OF MGO (TONS)	TOTAL CO_2 EMISSIONS (TONS)
47.59%	4144.95	0.00	0.00	3585.71	11868.82
	ANNUAL COST OF HYDROGEN ($)	ANNUAL COST OF NATURAL GAS ($)	ANNUAL COST OF METHANOL ($)	ANNUAL COST OF MGO ($)	TOTAL ANNUAL FUEL COST ($)
	10,362,364.19	0.00	0.00	2,294,853.02	12,657,217.21

6.7 2 COGES with Methanol and 1 9L46TS-DF with Natural Gas

The results of the case study scenario, which uses 2 COGES, with Methanol for fuel and 1L46TS-DF, with Natural Gas for fuel, as a propulsion plant during one year are illustrated in Table 31.

Table 31. Annual fuel consumption, total CO_2 emissions, total annual fuel cost for case 2 COGES with Methanol and 1 9L46TS-DF with Natural Gas

2 COGES WITH METHANOL AND 1 9L46TS-DF WITH NATURAL GAS					
AVERAGE $N_{OVERALL}$	ANNUAL CONS. OF HYDROGEN (TONS)	ANNUAL CONS. OF NATURAL GAS (TONS)	ANNUAL CONS. OF METHANOL (TONS)	ANNUAL CONS. OF MGO (TONS)	TOTAL CO_2 EMISSIONS (TONS)
47.10%	0.00	3076.24	25156.28	73.64	43622.77
	ANNUAL COST OF HYDROGEN ($)	ANNUAL COST OF NATURAL GAS ($)	ANNUAL COST OF METHANOL ($)	ANNUAL COST OF MGO ($)	TOTAL ANNUAL FUEL COST ($)
	0.00	3,383,859.68	11,320,325.76	47,129.50	14,751,314.94

6.8 2 COGES with Methanol and 1 9L46TS-DF with Methanol

The results of the case study scenario, which uses 2 COGES, with Methanol for fuel and 1L46TS-DF, with Methanol for fuel, as a propulsion plant during one year are illustrated in Table 32.

Table 32. Annual fuel consumption, total CO_2 emissions, total annual fuel cost for case 2 COGES with Methanol and 1 9L46TS-DF with Methanol

2 COGES WITH METHANOL AND 1 9L46TS-DF WITH METHANOL					
AVERAGE $N_{OVERALL}$	ANNUAL CONS. OF HYDROGEN (TONS)	ANNUAL CONS. OF NATURAL GAS (TONS)	ANNUAL CONS. OF METHANOL (TONS)	ANNUAL CONS. OF MGO (TONS)	TOTAL CO_2 EMISSIONS (TONS)
47.10%	0.00	0.00	32825.23	73.64	45674.24
	ANNUAL COST OF HYDROGEN ($)	ANNUAL COST OF NATURAL GAS ($)	ANNUAL COST OF METHANOL ($)	ANNUAL COST OF MGO ($)	TOTAL ANNUAL FUEL COST ($)
	0.00	0.00	14,771,354.46	47,129.50	14,818,483.96

6.9 2 COGES with Methanol and 1 9L46TS-DF with MGO

The results of the case study scenario, which uses 2 COGES, with Methanol for fuel and 1L46TS-DF, with MGO for fuel, as a propulsion plant during one year are depicted in Table 33.

Table 33. Annual fuel consumption, total CO_2 emissions, total annual fuel cost for case 2 COGES with Methanol and 1 9L46TS-DF with MGO

2 COGES WITH METHANOL AND 1 9L46TS-DF WITH MGO					
AVERAGE $N_{OVERALL}$	ANNUAL CONS. OF HYDROGEN (TONS)	ANNUAL CONS. OF NATURAL GAS (TONS)	ANNUAL CONS. OF METHANOL (TONS)	ANNUAL CONS. OF MGO (TONS)	TOTAL CO_2 EMISSIONS (TONS)
46.98%	0.00	0.00	25156.28	3634.46	46474.52
	ANNUAL COST OF HYDROGEN ($)	ANNUAL COST OF NATURAL GAS ($)	ANNUAL COST OF METHANOL ($)	ANNUAL COST OF MGO ($)	TOTAL ANNUAL FUEL COST ($)
	0.00	0.00	11,320,325.76	2,326,054.30	13,646,380.06

6.10 2 COGES with Natural Gas and 1 9L46TS-DF with Natural Gas

The results of the case study scenario, which uses 2 COGES, with Natural Gas for fuel and 1L46TS-DF, with Natural Gas for fuel, as a propulsion plant during one year are depicted in Table 34.

Table 34. Annual fuel consumption, total CO_2 emissions, total annual fuel cost for case 2 COGES with Natural Gas and 1 9L46TS-DF with Natural Gas

2 COGES WITH NATURAL GAS AND 1 9L46TS-DF WITH NATURAL GAS					
AVERAGE $N_{OVERALL}$	ANNUAL CONS. OF HYDROGEN (TONS)	ANNUAL CONS. OF NATURAL GAS (TONS)	ANNUAL CONS. OF METHANOL (TONS)	ANNUAL CONS. OF MGO (TONS)	TOTAL CO_2 EMISSIONS (TONS)
47.48%	0.00	12020.88	0.00	84.73	33737.80
	ANNUAL COST OF HYDROGEN ($)	ANNUAL COST OF NATURAL GAS ($)	ANNUAL COST OF METHANOL ($)	ANNUAL COST OF MGO ($)	TOTAL ANNUAL FUEL COST ($)
	0.00	13,222,971.24	0.00	54,229.77	13,277,201.01

6.11 2 COGES with Natural Gas and 1 9L46TS-DF with Methanol

The results of the case study scenario, which uses 2 COGES, with Natural Gas for fuel and 1L46TS-DF, with Methanol for fuel, as a propulsion plant during one year are depicted in Table 35.

Table 35. Annual fuel consumption, total CO_2 emissions, total annual fuel cost for case 2 COGES with Natural Gas and 1 9L46TS-DF with Methanol

2 COGES WITH NATURAL GAS AND 1 9L46TS-DF WITH METHANOL					
AVERAGE $N_{OVERALL}$	ANNUAL CONS. OF HYDROGEN (TONS)	ANNUAL CONS. OF NATURAL GAS (TONS)	ANNUAL CONS. OF METHANOL (TONS)	ANNUAL CONS. OF MGO (TONS)	TOTAL CO_2 EMISSIONS (TONS)
47.48%	0.00	8369.85	9101.91	84.73	36172.58
	ANNUAL COST OF HYDROGEN ($)	ANNUAL COST OF NATURAL GAS ($)	ANNUAL COST OF METHANOL ($)	ANNUAL COST OF MGO ($)	TOTAL ANNUAL FUEL COST ($)
	0.00	9,206,831.61	4,095,859.30	54,229.77	13,356,920.68

6.12 2 COGES with Natural Gas and 1 9L46TS-DF with MGO

The results of the case study scenario, which uses 2 COGES, with Natural Gas for fuel and 1L46TS-DF, with MGO for fuel, as a propulsion plant during one year are depicted in Table 36.

Table 36. Annual fuel consumption, total CO2 emissions, total annual fuel cost for case 2 COGES with Natural Gas and 1 9L46TS-DF with MGO

2 COGES WITH NATURAL GAS AND 1 9L46TS-DF WITH MGO					
AVERAGE $N_{OVERALL}$	ANNUAL CONS. OF HYDROGEN (TONS)	ANNUAL CONS. OF NATURAL GAS (TONS)	ANNUAL CONS. OF METHANOL (TONS)	ANNUAL CONS. OF MGO (TONS)	TOTAL CO_2 EMISSIONS (TONS)
47.35%	0.00%	8369.85	0.00	4316.83	37141.41
	ANNUAL COST OF HYDROGEN($)	ANNUAL COST OF NATURAL GAS ($)	ANNUAL COST OF METHANOL ($)	ANNUAL COST OF MGO ($)	TOTAL ANNUAL FUEL COST ($)
	0.00	9,206,831.61	0.00	2,762,770.16	11,969,601.77

6.13 2 COGES with a mixture of 70% Hydrogen - 30% Natural Gas and 1 9L46TS-DF with Natural Gas

The results of the case study scenario, which uses 2 COGES, with a mixture of 70% Hydrogen - 30% Natural Gas for fuel and 1L46TS-DF, with Natural Gas for fuel, as a propulsion plant during one year are depicted in Table 37.

Table 37. Annual fuel consumption, total CO_2 emissions, total annual fuel cost for case 2 COGES a mixture of 70% Hydrogen - 30% Natural Gas and 1 9L46TS-DF with Natural Gas

2 COGES WITH A MIXTURE OF 70% Hydrogen - 30% Natural Gas and 1 9L46TS-DF WITH NATURAL GAS					
ΜΕΣΟΣ Β.Α.	ΣΥΝΟΛΙΚΗ ΚΑΤΑΝΑΛΩΣΗ HYDR ΕΤΗΣΙΩΣ(TONS)	ΣΥΝΟΛΙΚΗ ΚΑΤΑΝΑΛΩΣΗ NG ΕΤΗΣΙΩΣ(TONS)	ΣΥΝΟΛΙΚΗ ΚΑΤΑΝΑΛΩΣΗ METH ΕΤΗΣΙΩΣ(TONS)	ΣΥΝΟΛΙΚΗ ΚΑΤΑΝΑΛΩΣΗ PO ΕΤΗΣΙΩΣ(TONS)	ΣΥΝΟΛΙΚΕΣ ΕΚΠΟΜΠΕΣ CO2(TONS)
47.56%	3344.09	5084.22	0.00	84.73	14727.08
	ΣΥΝΟΛΙΚΟ ΚΟΣΤΟΣ HYDR($)	ΣΥΝΟΛΙΚΟ ΚΟΣΤΟΣ NG($)	ΣΥΝΟΛΙΚΟ ΚΟΣΤΟΣ METHANOL($)	ΣΥΝΟΛΙΚΟ ΚΟΣΤΟΣ FO($)	ΣΥΝΟΛΙΚΟ ΚΟΣΤΟΣ($)
	8,360,220.94	5,592,638.44	0.00	54,229.77	14,007,089.15

6.14 2 COGES with a mixture of 70% Hydrogen - 30% Natural Gas and 1 9L46TS-DF with Methanol

The results of the case study scenario, which uses 2 COGES, with a mixture of 70% Hydrogen - 30% Natural Gas for fuel and 1L46TS-DF, with Methanol for fuel, as a propulsion plant during one year are depicted in Table 38.

Table 38. Annual fuel consumption, total CO_2 emissions, total annual fuel cost for case 2 COGES a mixture of 70% Hydrogen - 30% Natural Gas and 1 9L46TS-DF with Methanol

2 COGES WITH A MIXTURE OF 70% Hydrogen - 30% Natural Gas and 1 9L46TS-DF WITH METHANOL					
AVERAGE $N_{OVERALL}$	ANNUAL CONS. OF HYDROGEN (TONS)	ANNUAL CONS. OF NATURAL GAS (TONS)	ANNUAL CONS. OF METHANOL (TONS)	ANNUAL CONS. OF MGO (TONS)	TOTAL CO_2 EMISSIONS (TONS)
47.56%	3344.09	1433.18	9101.91	84.73	17161.87
	ANNUAL COST OF HYDROGEN ($)	ANNUAL COST OF NATURAL GAS ($)	ANNUAL COST OF METHANOL ($)	ANNUAL COST OF MGO ($)	TOTAL ANNUAL FUEL COST ($)
	8,360,220.94	1,576,498.81	4,095,859.30	54,229.77	14,086,808.81

6.15 2 COGES with a mixture of 70% Hydrogen - 30% Natural Gas and 1 9L46TS-DF with MGO

The results of the case study scenario, which uses 2 COGES, with a mixture of 70% Hydrogen - 30% Natural Gas for fuel and 1L46TS-DF, with MGO for fuel, as a propulsion plant during one year are depicted in Table 39.

Table 39. Annual fuel consumption, total CO_2 emissions, total annual fuel cost for case 2 COGES a mixture of 70% Hydrogen - 30% Natural Gas and 1 9L46TS-DF with MGO

2 COGES WITH A MIXTURE OF 70% Hydrogen - 30% Natural Gas and 1 9L46TS-DF WITH MGO					
AVERAGE $N_{OVERALL}$	ANNUAL CONS. OF HYDROGEN (TONS)	ANNUAL CONS. OF NATURAL GAS (TONS)	ANNUAL CONS. OF METHANOL (TONS)	ANNUAL CONS. OF MGO (TONS)	TOTAL CO_2 EMISSIONS (TONS)
47.43%	3344.09	1433.18	0.00	4316.83	18130.69
	ANNUAL COST OF HYDROGEN ($)	ANNUAL COST OF NATURAL GAS ($)	ANNUAL COST OF METHANOL ($)	ANNUAL COST OF MGO ($)	TOTAL ANNUAL FUEL COST ($)
	8,360,220.94	1,576,498.81	0.00	2,762,770.16	12,699,489.90

6.16 2 COGES with a mixture of 80% Hydrogen - 20% Natural Gas and 1 9L46TS-DF with Natural Gas

The results of the case study scenario, which uses 2 COGES, with a mixture of 80% Hydrogen - 20% Natural Gas for fuel and 1L46TS-DF, with Natural Gas for fuel, as a propulsion plant during one year are depicted in Table 40.

Table 40. Annual fuel consumption, total CO_2 emissions, total annual fuel cost for case 2 COGES a mixture of 80% Hydrogen - 20% Natural Gas and 1 9L46TS-DF with Natural Gas

2 COGES WITH A MIXTURE OF 80% Hydrogen - 20% Natural Gas and 1 9L46TS-DF WITH NATURAL GAS					
AVERAGE $N_{OVERALL}$	ANNUAL CONS. OF HYDROGEN (TONS)	ANNUAL CONS. OF NATURAL GAS (TONS)	ANNUAL CONS. OF METHANOL (TONS)	ANNUAL CONS. OF MGO (TONS)	TOTAL CO_2 EMISSIONS (TONS)
47.55%	3576.98	4545.28	0.00	84.73	13247.64
	ANNUAL COST OF HYDROGEN($)	ANNUAL COST OF NATURAL GAS ($)	ANNUAL COST OF METHANOL ($)	ANNUAL COST OF MGO ($)	TOTAL ANNUAL FUEL COST ($)
	8,942,439.87	4,999,808.02	0.00	54,229.77	13,996,477.66

6.17 2 COGES with a mixture of 80% Hydrogen - 20% Natural Gas and 1 9L46TS-DF with Methanol

The results of the case study scenario, which uses 2 COGES, with a mixture of 80% Hydrogen - 20% Natural Gas for fuel and 1L46TS-DF, with Methanol for fuel, as a propulsion plant during one year are depicted in Table 41.

Table 41. Annual fuel consumption, total CO_2 emissions, total annual fuel cost for case 2 COGES a mixture of 80% Hydrogen - 20% Natural Gas and 1 9L46TS-DF with Methanol

2 COGES WITH A MIXTURE OF 80% Hydrogen - 20% Natural Gas and 1 9L46TS-DF WITH METHANOL					
AVERAGE $N_{OVERALL}$	ANNUAL CONS. OF HYDROGEN (TONS)	ANNUAL CONS. OF NATURAL GAS (TONS)	ANNUAL CONS. OF METHANOL (TONS)	ANNUAL CONS. OF MGO (TONS)	TOTAL CO_2 EMISSIONS (TONS)
47.55%	3576.98	894.24	9101.91	84.73	15682.43
	ANNUAL COST OF HYDROGEN ($)	ANNUAL COST OF NATURAL GAS ($)	ANNUAL COST OF METHANOL ($)	ANNUAL COST OF MGO ($)	TOTAL ANNUAL FUEL COST ($)
	8942439.87	983,668.39	4,095,859.30	54,229.77	14,076,197.33

6.18 2 COGES with a mixture of 80% Hydrogen - 20% Natural Gas and 1 9L46TS-DF with MGO

The results of the case study scenario, which uses 2 COGES, with a mixture of 80% Hydrogen - 20% Natural Gas for fuel and 1L46TS-DF, with MGO for fuel, as a propulsion plant during one year are depicted in Table 42.

Table 42. Annual fuel consumption, total CO_2 emissions, total annual fuel cost for case 2 COGES a mixture of 80% Hydrogen - 20% Natural Gas and 1 9L46TS-DF with MGO

2 COGES WITH A MIXTURE OF 80% Hydrogen - 20% Natural Gas and 1 9L46TS-DF WITH MGO					
AVERAGE $N_{OVERALL}$	ANNUAL CONS. OF HYDROGEN (TONS)	ANNUAL CONS. OF NATURAL GAS (TONS)	ANNUAL CONS. OF METHANOL (TONS)	ANNUAL CONS. OF MGO (TONS)	TOTAL CO_2 EMISSIONS (TONS)
47.42%	3576.98	894.24	0.00	4316.83	16651.25
	ANNUAL COST OF HYDROGEN ($)	ANNUAL COST OF NATURAL GAS ($)	ANNUAL COST OF METHANOL ($)	ANNUAL COST OF MGO ($)	TOTAL ANNUAL FUEL COST ($)
	8,942,439.87	983,668.39	0.00	2,762,770.16	12,688,878.42

6.19 Diagrammatic Illustration of the Case Study Scenarios

The aggregated data will be presented below in common charts for all case study scenarios. First, the annual fuel cost is depicted in photo 19. It is understood that when using conventional diesel engines with diesel fuel, the cost is significantly lower than all other scenarios based on the obtained fuel prices. For this reason, greater weight will be given to the analysis of the remaining scenarios, in which alternative fuels are used purely or in combination with diesel oil. The highest fuel cost is observed in cases 07 and 08 and is almost 14,800,000$. These cases use methanol-fueled COGES and methanol-fueled and natural gas-fired conventional diesel engines. The lowest fuel cost is observed in case 12, which is almost 12,000,000$. The case uses COGES fueled by natural gas and conventional diesel engines fueled by fuel oil.

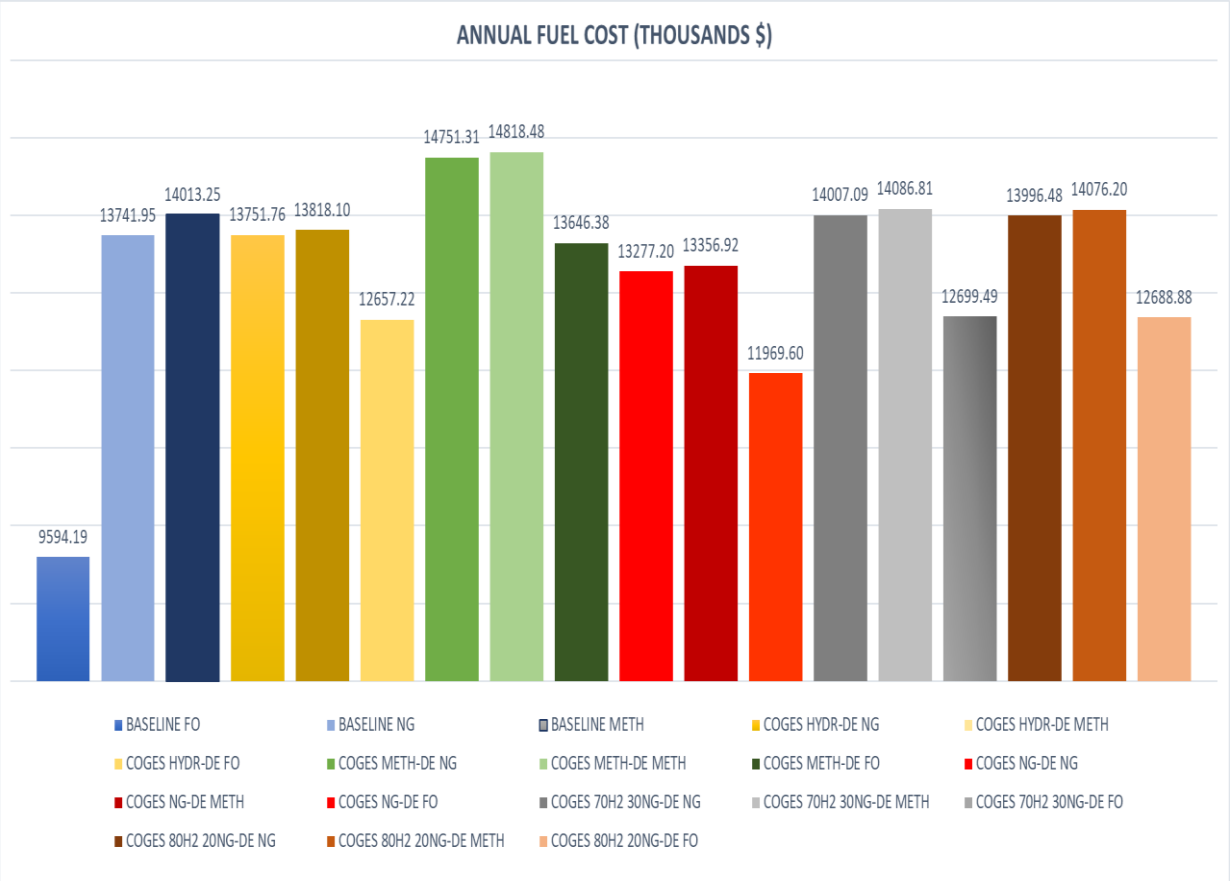

Figure 19. Annual Fuel Cost of all the studied Scenarios

The results of Figure 19 are best understood in Figure 20 which shows the percentage change in annual fuel costs compared to scenario 02 where conventional gas-fired diesel engines are used. In particular, COGES significantly contributes to increasing gas turbine efficiency as most scenarios are either at the same level or have lower fuel costs compared to conventional diesel engines. In scenario 12 the annual savings reach $ 1,800.00 while in the immediate best scenario, case 06, the savings reach $ 1,100,000 and hydrogen with zero environmental footprint is used.

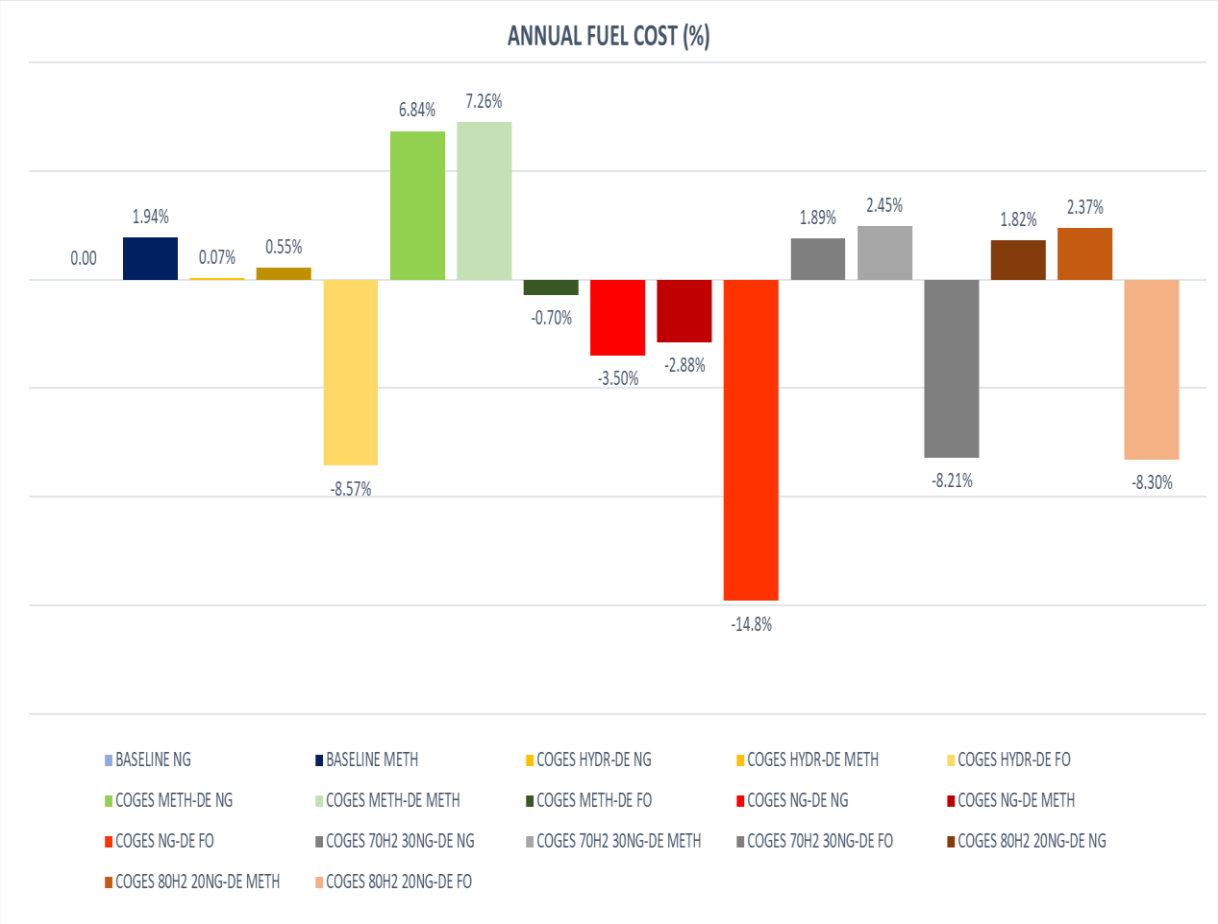

Figure 20. Annual Fuel Cost of all the studied Scenarios compared to the Case 02

Concerning CO2 emissions, the results are shown in Figures 21 and 22. The highest levels of emissions are observed when fuel oil and methanol are used as main fuel. At lower emission levels are cases where natural gas is the main fuel, while the rapid reduction of emissions is observed when hydrogen or mixtures containing hydrogen are used as the main fuel. In particular, compared to the scenario of using conventional gas-fired diesel engines, the scenarios using hydrogen-fuelled COGES show a reduction in CO_2 emissions of more than 195%. In addition, the COGES scenarios using a mixture of hydrogen and natural gas as fuel, the emission reduction compared to scenario 02 ranges from 90% to 164%.

Figure 21. Annual CO_2 Emissions of all the studied Scenarios

Figure 22. Annual CO_2 Emissions of all the studied Scenarios compared to the Case 02

In conclusion, at fuel cost levels, conventional engines using diesel oil as fuel cannot be compared with the rest of the examined scenarios. However, the above figures strongly demonstrate the ability of COGES to make gas turbine use economically viable and in many cases better in cost terms than conventional diesel engines using alternative fuels. Also, the COGES system, due to its flexibility in the use of alternative fuels, has the potential to rapidly reduce carbon dioxide emissions and make the ships that use it environmentally friendly.

7. Conclusions

The study was motivated by a need to reduce emissions in marine transport, influenced by international environmental standards. Traditional propulsion methods struggle to meet these new requirements, directing attention to innovative technologies such as Combined Gas Electric and Steam (COGES) systems, which combine gas and steam turbines for increased efficiency and reduced emissions. COGES systems promise high thermal performance, especially with low-carbon fuels, and represent a step forward in sustainable marine engineering. By using thermodynamic modeling and the creation of a thermal analysis correlation, it was possible to establish direct calculations of the heat transfer coefficient at partial loads without repeated in-depth analysis. This correlation was applied by measuring exhaust gas temperatures and mass supply at full load, which then enabled the prediction of the total heat transfer coefficient at 50-90% loads with minimal error (under 0.5%), showcasing a high degree of accuracy in modeling efforts. The study also aimed to model and optimize a COGES system on a cruise ship. This involved calculating fuel efficiency and emissions reductions across load scenarios and fuel types. Through this process, the study illustrated that COGES achieves up to 50% efficiency and can reduce emissions significantly. Moreover, a case study for a modern cruise ship using conventional diesel engines and COGES was carried out. The usage plan of the engines for the cruise ship was created based on its power demands on an annual basis. This usage plan outlined in the study ensures that COGES operates efficiently alongside diesel engines. When power demands did not reach 70% of one COGES unit or exceeded 70% of a single unit, a diesel engine would supplement the system. When both COGES units were in use, load distribution was equalized to maintain operation below 95% of maximum continuous rating (MCR). This plan enables the system to maintain high efficiency while managing varying load demands. In this case study, hydrogen-powered configurations demonstrated up to a 195% reduction in CO_2 emissions relative to conventional diesel engines, while the optimized COGES design significantly reduced fuel use costs comparative to diesel engines with alternative fuels. In conclusion, the findings strongly support the necessity of adopting COGES systems. This study shows that COGES not only meets but exceeds emissions requirements, presenting an effective solution for the environmental and operational demands of modern marine vessels.

Bibliography

[1] ‘LOGISTICS, D.O.T.AND.U.N.C.O.T.A.D., 2022. REVIEW OF MARITIME TRANSPORT 2021. UNITED NATIONS, S.l.’

[2] T. W. P. Smith *et al.*, ‘Third IMO Greenhouse Gas Study 2014’, Apr. 2015, Accessed: Sep. 24, 2024. [Online]. Available: https://research.manchester.ac.uk/en/publications/third-imo-greenhouse-gas-study-2014

[3] T.-H. Joung, S.-G. Kang, J.-K. Lee, and J. Ahn, ‘The IMO initial strategy for reducing Greenhouse Gas(GHG) emissions, and its follow-up actions towards 2050’, *J. Int. Marit. Saf. Environ. Aff. Shipp.*, vol. 4, no. 1, pp. 1–7, Jan. 2020, doi: 10.1080/25725084.2019.1707938.

[4] ‘Rules on ship carbon intensity and rating system enter into force’. Accessed: Sep. 24, 2024. [Online]. Available: https://www.imo.org/en/MediaCentre/PressBriefings/pages/CII-and-EEXI-entry-into-force.aspx

[5] G. Mallouppas and E. Ar. Yfantis, ‘Decarbonization in Shipping Industry: A Review of Research, Technology Development, and Innovation Proposals’, *J. Mar. Sci. Eng.*, vol. 9, no. 4, p. 415, Apr. 2021, doi: 10.3390/jmse9040415.

[6] O. B. Inal, B. Zincir, and C. Deniz, ‘Investigation on the decarbonization of shipping: An approach to hydrogen and ammonia’, *Int. J. Hydrog. Energy*, vol. 47, no. 45, pp. 19888–19900, May 2022, doi: 10.1016/j.ijhydene.2022.01.189.

[7] K. Cullinane and J. Yang, ‘Evaluating the Costs of Decarbonizing the Shipping Industry: A Review of the Literature’, *J. Mar. Sci. Eng.*, vol. 10, no. 7, Art. no. 7, Jul. 2022, doi: 10.3390/jmse10070946.

[8] A. Christodoulou, D. Dalaklis, A. I. Ölçer, and P. Ghaforian Masodzadeh, ‘Inclusion of Shipping in the EU-ETS: Assessing the Direct Costs for the Maritime Sector Using the MRV Data’, *Energies*, vol. 14, no. 13, Art. no. 13, Jan. 2021, doi: 10.3390/en14133915.

[9] H. Jouhara, N. Khordehgah, S. Almahmoud, B. Delpech, A. Chauhan, and S. A. Tassou, ‘Waste heat recovery technologies and applications’, *Therm. Sci. Eng. Prog.*, vol. 6, pp. 268–289, Jun. 2018, doi: 10.1016/j.tsep.2018.04.017.

[10] F. Baldi and C. Gabrielii, ‘A feasibility analysis of waste heat recovery systems for marine applications’, *Energy*, vol. 80, pp. 654–665, Feb. 2015, doi: 10.1016/j.energy.2014.12.020.

[11] D. V. Singh and E. Pedersen, ‘A review of waste heat recovery technologies for maritime applications’, *Energy Convers. Manag.*, vol. 111, pp. 315–328, Mar. 2016, doi: 10.1016/j.enconman.2015.12.073.

[12] S. Suárez de la Fuente and A. R. Greig, ‘Making shipping greener: comparative study between organic fluids and water for Rankine cycle waste heat recovery’, *J. Mar. Eng. Technol.*, vol. 14, no. 2, pp. 70–84, May 2015, doi: 10.1080/20464177.2015.1077601.

[13] M. A. Budiyanto *et al.*, 'Techno-Economic Analysis of Combined Gas and Steam Propulsion System of Liquefied Natural Gas Carrier', *Energies*, vol. 17, no. 6, Art. no. 6, Jan. 2024, doi: 10.3390/en17061415.

[14] A. Dotto, R. Sacchi, F. Satta, and U. Campora, 'Dynamic performance simulation of combined gas electric and steam power plants for cruise-ferry ships', *Energy*, vol. 1, no. 3, p. 100020, Sep. 2023, doi: 10.1016/j.nxener.2023.100020.

[15] A. Dotto, U. Campora, and F. Satta, 'Feasibility study of an integrated COGES-DF engine power plant in LNG propulsion for a cruise-ferry', *Energy Convers. Manag.*, vol. 245, p. 114602, Oct. 2021, doi: 10.1016/j.enconman.2021.114602.

[16] W. Nirbito, M. A. Budiyanto, and R. Muliadi, 'Performance Analysis of Combined Cycle with Air Breathing Derivative Gas Turbine, Heat Recovery Steam Generator, and Steam Turbine as LNG Tanker Main Engine Propulsion System', *J. Mar. Sci. Eng.*, vol. 8, no. 9, p. 726, Sep. 2020, doi: 10.3390/jmse8090726.

[17] M. Dzida and W. Olszewski, 'Comparing combined gas tubrine/steam turbine and marine low speed piston engine/steam turbine systems in naval applications', *Pol. Marit. Res.*, vol. 18, no. 4, pp. 43–48, Jan. 2011, doi: 10.2478/v10012-011-0025-8.

[18] M. Altosole, U. Campora, and S. Savio, 'Improvements of the Ship Energy Efficiency by a Steam Powered Turbogenerator in LNG Propulsion Applications', in *2018 International Symposium on Power Electronics, Electrical Drives, Automation and Motion (SPEEDAM)*, Amalfi: IEEE, Jun. 2018, pp. 449–455. doi: 10.1109/SPEEDAM.2018.8445202.

[19] J. Ahn, S. Lee, J. Jeong, and Y. Choi, 'Comparative feasibility study of combined cycles for marine power system in a large container ship considering energy efficiency design index (EEDI)', *Int. J. Hydrog. Energy*, vol. 46, no. 62, pp. 31816–31827, Sep. 2021, doi: 10.1016/j.ijhydene.2021.07.068.

[20] F. Haglind, 'A review on the use of gas and steam turbine combined cycles as prime movers for large ships. Part I: Background and design', *Energy Convers. Manag.*, vol. 49, no. 12, pp. 3458–3467, Dec. 2008, doi: 10.1016/j.enconman.2008.08.005.

[21] L. Ellington, G. McAndrews, A. Harsema-Mensonides, and R. Tanwar, 'Gas Turbine Propulsion for LNG Transports', in *Volume 5: Marine; Microturbines and Small Turbomachinery; Oil and Gas Applications; Structures and Dynamics, Parts A and B*, Barcelona, Spain: ASMEDC, Jan. 2006, pp. 65–76. doi: 10.1115/GT2006-90715.

[22] A. Armellini, S. Daniotti, and P. Pinamonti, 'Gas Turbines for Power Generation on Board of Cruise Ships: A Possible Solution to Meet the New IMO Regulations?', *Energy Procedia*, vol. 81, pp. 540–547, Dec. 2015, doi: 10.1016/j.egypro.2015.12.127.

[23] A. I. Sayma, 'Gas Turbines for Marine Applications', in *Encyclopedia of Maritime and Offshore Engineering*, 1st ed., J. Carlton, P. Jukes, and Y. S. Choo, Eds., Wiley, 2017, pp. 1–10. doi: 10.1002/9781118476406.emoe227.

[24] D. Barsi, M. Luzzi, F. Satta, and P. Zunino, ‘On the Possible Introduction of Mini Gas Turbine Cycles Onboard Ships for Heat and Power Generation’, *Energies*, vol. 14, no. 3, p. 568, Jan. 2021, doi: 10.3390/en14030568.

[25] A. Dotto, U. Campora, and F. Satta, ‘Feasibility study of an integrated COGES-DF engine power plant in LNG propulsion for a cruise-ferry’, *Energy Convers. Manag.*, vol. 245, p. 114602, Oct. 2021, doi: 10.1016/j.enconman.2021.114602.

[26] J. Larfeldt, ‘Technology options and plant design issues for fuel-flexible gas turbines’, in *Fuel Flexible Energy Generation*, Elsevier, 2016, pp. 271–291. doi: 10.1016/B978-1-78242-378-2.00010-9.

[27] M. Moliere, ‘Expanding fuel flexibility of gas turbines’, *Proc. Inst. Mech. Eng. Part J. Power Energy*, vol. 219, no. 2, pp. 109–119, Mar. 2005, doi: 10.1243/095765005X6818.

[28] M. Welch, B. M. Igoe, and D. Wilson, ‘Combustion, Fuels and Emissions for Industrial Gas Turbines’, 2016, Accessed: Sep. 25, 2024. [Online]. Available: https://hdl.handle.net/1969.1/160298

[29] M. Stefanizzi, T. Capurso, G. Filomeno, M. Torresi, and G. Pascazio, ‘Recent Combustion Strategies in Gas Turbines for Propulsion and Power Generation toward a Zero-Emissions Future: Fuels, Burners, and Combustion Techniques’, *Energies*, vol. 14, no. 20, p. 6694, Oct. 2021, doi: 10.3390/en14206694.

[30] I. I. Enagi, K. A. Al-attab, and Z. A. Zainal, ‘Liquid biofuels utilization for gas turbines: A review’, *Renew. Sustain. Energy Rev.*, vol. 90, pp. 43–55, Jul. 2018, doi: 10.1016/j.rser.2018.03.006.

[31] C. Ghenai, ‘Combustion of Syngas Fuel in Gas Turbine Can Combustor’, *Adv. Mech. Eng.*, vol. 2, p. 342357, Jan. 2010, doi: 10.1155/2010/342357.

[32] P. J. Dechamps and J.-F. Galopin, ‘Once-Through Heat Recovery Steam Generators Working With Sub- and Supercritical Steam Conditions for Combined Cycles’, in *Volume 3: Heat Transfer; Electric Power; Industrial and Cogeneration*, Orlando, Florida, USA: American Society of Mechanical Engineers, Jun. 1997, p. V003T10A006. doi: 10.1115/97-GT-337.

[33] E. Næss, ‘Experimental investigation of heat transfer and pressure drop in serrated-fin tube bundles with staggered tube layouts’, *Appl. Therm. Eng.*, vol. 30, no. 13, pp. 1531–1537, Sep. 2010, doi: 10.1016/j.applthermaleng.2010.02.019.

[34] S. M. Ammar and C. W. Park, ‘Validation of the Gnielinski correlation for evaluation of heat transfer coefficient of enhanced tubes by non-linear regression model: An experimental study of absorption refrigeration system’, *Int. Commun. Heat Mass Transf.*, vol. 118, p. 104819, Nov. 2020, doi: 10.1016/j.icheatmasstransfer.2020.104819.

[35] E. Cao, *Heat Transfer in Process Engineering*, 1st edition. Champaign, Ill.: McGraw Hill, 2009.